Downloaded from rstb.royalsocietypublishing.org

PHILOSOPHICAL TRANSACTIONS OF THE ROYAL SOCIETY B BIOLOGICAL SCIENCES

Biomass Production, Structural Deformation, Self-Thinning and Thinning Mechanisms in Monocultures

F. M. Burrows

Phil. Trans. R. Soc. Lond. B 1991 **333**, 119-145
doi: 10.1098/rstb.1991.0064

Email alerting service

Receive free email alerts when new articles cite this article - sign up in the box at the top right-hand corner of the article or click **here**

To subscribe to *Phil. Trans. R. Soc. Lond. B* go to: **http://rstb.royalsocietypublishing.org/subscriptions**

This journal is © 1991 The Royal Society

Downloaded from rstb.royalsocietypublishing.org

Biomass production, structural deformation, self-thinning and thinning mechanisms in monocultures

F. M. BURROWS†

Department of Mathematics, Westminster School, 17 Dean's Yard, London SW1P 3PB, U.K.; University College of North Wales, Bangor, Gwynedd LL57 2DG, U.K.

CONTENTS

SUMMARY

Consideration is given to the production of biomass in three of the possible growth phases that may be experienced by plants at various spacings in stand monocultures. The amount of radiant energy available for this is related to canopy surface area, volume, and slenderness, and the efficiency with which the operation is performed. The unified non-dimensional formulae established describe normal natural growth, growth with plastic deformation, and growth subject to the self-thinning process, which occurs when individuals are packed too closely together. The formulae define growth surfaces for the life-lines followed by individual plants, and for the rounding and smoothing of these lines that occurs, at the otherwise sharply defined growth phase boundaries, as a result of the statistical uncertainties in specifying plant dimensions and numbers in spacetime. The results provide an explanation of features of the self-thinning process and the values of the constants and parameters associated with approximate power law descriptions of the phase boundary on which it takes place. A quasi-static analysis of growth and thinning mechanisms indicates one-sided competition coexistence conditions for plants in distributions with uniformly augmented and diminished biomass, and the boundaries separating and distinguishing diminished biomass states from which recovery to further growth is, or is not, possible. Because of the dependence of events in the growth process on canopy shape and volume a preliminary classification of suitable geometric forms is given, together with formulae for evaluating the required quantities, for several cases of interest.

NOMENCLATURE

a, b	constant and index in power law $M = aX^b$
A, B, C	terms in logarithmic form of the biomass equation (62). In Appendix 2, A is used to denote a specified area
C_p	packing coefficient defined as the ratio of plant cylinder area to the area of ground available to accommodate it
$E[X(\tau)]$	expected value of X at time τ
$E[\mu(\tau, X)]$	expected value of μ at time τ and given X

† Current address: Department of Computing and Information Systems, City of London Polytechnic, 100 Minories, Tower Hill, London EC3N 1JY, U.K.

Printed in Great Britain

The Royal Society is collaborating with JSTOR to digitize, preserve, and extend access to *Philosophical Transactions: Biological Sciences.* www.jstor.org

Downloaded from rstb.royalsocietypublishing.org

$F(t)$ function representing fertility and nutrient availability at time t
F_1, F_2 monovariate and bivariate Gaussian probability density functions (equations (A 3.1, A 3.2))
H, H_∞ height of plant and solar cylinders at time t, and at full growth
H_0, H_1 plant canopy envelope height coordinates (Appendix 1)
k number of plants in augmented growth with mass μ_a at time t
k^* number of plants on the definitive growth limit boundary
k_0 radiation diffusion coefficient (Appendix 2)
K_0 coefficient describing the undersurface contribution to canopy surface area S
M, M_c, M_s biomass produced by radiation within the plant canopy, the plant cylinder, and the solar cylinder at time t
M_∞ total biomass that could be produced within the solar cylinder under perfect conditions of fertility and nutrient supply
M_g biomass produced per unit area of ground
M_1, M_2 quantities used in evaluating the non-dimensional radial distances from the centre of the solar cylinder to the centre of an arbitrary plant cylinder (Appendix 2)
m, n positive integers (Appendix 2)
n number of plants of different sizes in the solar cylinder at a given time (equation (42))
N_g number of solar cylinders accommodated on ground area S_g
p, q indices in the differential equations for growth (17). In Appendix 2, $p = \lambda_r M_\alpha$, $q = (1+p^2-\lambda_r^2)/(2p)$, $\alpha = 1, 2$
$r_\alpha = qR_\infty$ Appendix 2
R radius of plant cylinder at time t
R_∞ radius of solar cylinder and radius of plant cylinder at full growth
R_0, R_1 plant canopy envelope radial coordinates (Appendix 2)
S effective surface area of plant canopy envelope
S_c surface area of plant cylinder above ground
S_g arbitrary ground reference area
S_s surface area of solar cylinder above ground
S_0, S_m, S_n numbers of whole plant cylinders used for the calculation of packing coefficients C_p
$s_\alpha = \pm(1-q^2)^{\frac{1}{2}}R_\infty$ (Appendix 2)
t real time
$t_{\frac{1}{2}}$ plant half-life time
$u = q-p$ Appendix 2
$v = u/\lambda_r$ Appendix 2
V plant canopy volume
V_c, V_s volume of plant and solar cylinders at time t
x, y plant radial and vertical coordinates
X number of plant cylinders within the solar cylinder at time t
X_0 initial planting density
X_p value of X on the plastic line
X_t value of X on the self-thinning line
X_2 dummy variable of integration (equations (A 3.2))
Y_1, Y_2, Y_3 independent variables in the dimensional biomass equation (62)
Z_1, Z_2, Z_3 dependent variables in the dimensional biomass equation (62)
$\alpha_a, \alpha_h, \alpha_m$ coefficients in the non-dimensional growth equations (23), (28), (47)
β coefficient in the differential equation for growth (17)
$\beta_a, \beta_h, \beta_m$ coefficients in the non-dimensional growth equations (23), (28), (47)
γ_h, γ_m exponents in the non-dimensional growth equations (23, 28)
$\theta = 1/(\theta_1+2)$
$\theta_1 = \lambda_\infty \lambda_r/\lambda_h = (\lambda_\infty/\lambda_h)(C_p/X_t)^{\frac{1}{2}}$
$\eta = y/H$
$\eta_0 = H_0/H$
$\lambda = R/H$
λ_h, λ_{h0} relative height H/H_∞ at time t and at $t = 0$
λ_r, λ_{r0} relative radius R/R_∞ at time t and at $t = 0$
λ_∞ plant slenderness ratio R_∞/H_∞
$\lambda_{\infty 1}, \lambda_{\infty 2}$ values of λ_∞ for two comparative cases (equation (66))
$\Lambda = (S/S_c)(V/V_c)$ canopy shape parameter
$\mu_{1,2,3} = M/(M_\infty \sigma \Lambda)$ unified non-dimensional biomass ratio at time t, with the suffices 1, 2, 3, denoting the growth phases
μ_0 value of $\mu_{1,2,3}$ at $t = 0$
$\mu_a, \mu_d, \mu_j, \mu_m$ augmented, diminished, individual, and mean non-dimensional biomass ratios in binary growth
μ_{a0}, μ_{a1} value of μ_a at $\tau = 0$ and $\tau = 1$

Downloaded from rstb.royalsocietypublishing.org

$\mu_s = n\mu_m$ non-dimensional biomass ratio for solar cylinder containing n plants
μ_{al}, μ_{sl} non-dimensional augmented and solar cylinder biomasses defining the definitive growth limit boundary
$\xi = x/R$
$\rho, \rho_c, \rho_s, \rho_\infty$ mean biomass densities for biomass produced within the canopy envelope, the plant cylinder, the solar cylinder, and in the solar cylinder under perfect conditions
τ non-dimensional time
τ_{mort} non-dimensional absolute growth limit time
τ_u, τ_l upper and lower limits for τ (equation (32))
τ_1, τ_2 dummy variables of integration (equations (A 3.1, A 3.2)
ϕ, ϕ_c, ϕ_s radiant energy flux received on the canopy envelope, the plant cylinder, and the solar cylinder at time t
$\sigma = \rho_s/\rho_\infty$ biomass density ratio

INTRODUCTION

When plants are growing together in a stand the physical effects of direct and indirect mutual interference to the growth process are such that it is possible to identify at least three distinct phases during the life-cycle of individuals in the community. These phases have been reported extensively for monocultures (Kira *et al.* 1953; Shinozaki & Kira 1956; Takadi & Shidei 1959; Harper 1977; White 1980, 1981) and, to a lesser though still significant extent, for multicultures (White & Harper 1970; Kays & Harper 1974; Bazzaz & Harper 1976; White 1980, 1981; Malmberg & Smith 1982). In the first of the phases each plant has sufficient space in which to develop and lay sole claim to the available energy and nutrients it needs for unrestricted growth; if the initial sowing is sparse, this state of affairs may exist for a considerable fraction of its life-span. The second phase is reached when the energy and nutrient input becomes less than that needed to support further unrestricted growth; although this does not mean that plants are crowded in the physical sense, the effect is apparently to engender a process of self-regulatory reduction in the size and mass of individuals. This is a plastic response, and it occasionally induces mortality (Kira *et al.* 1953; Harper 1967; White 1981). At later times, when contact is established between canopies, the growth pattern enters a third phase in which some of the plants die off as a result of competing unsuccessfully for the available space and resources. This process of self-thinning (Takadi & Shidei 1959; Yoda *et al.* 1963; Harper 1977; Gorham 1979; White 1981; Weller 1987) is a dominant feature of further growth to maturity of the diminishing population of a stand whose members may, in some cases, have markedly different mass and geometry from those enjoying the unrestricted growth conditions of Phase I. In mature stands a fourth phase may become established, in which individuals produce and lose biomass simultaneously, but this equilibrium condition is not considered here.

The third phase of growth has been described as following a *minus* $\frac{3}{2}$ *thinning rule* (Takadi & Shidei 1959; Yoda *et al.* 1963; White & Harper 1970; Watkinson 1980; Hutchings & Budd 1981; White 1981; Lonsdale & Watkinson 1982; Hutchings 1983; Pickard 1983; Charles-Edwards 1984*b*; Pahor 1985; Givinish 1986; Westoby 1984; Weller 1987; Lonsdale 1990), so named because of the slope apparently defined in logarithmic plots of biomass versus planting density, or similar variables representing these quantities. As derived initially by Yoda *et al.* (1963), this empirical rule was evidently in agreement with the power law they obtained in an analysis which related the area of ground covered by a plant canopy to the total dry biomass produced. It was based on the principle of geometric similarity, with area and volume assumed proportional to the square and cube respectively of a single characteristic linear dimension. It is of doubtful value on at least two counts: first, because it provides little evidence of the factors contributing to the composition of the rule as such (see, for example, Yoda *et al.* 1963; White 1981; Weller 1987); and secondly, because of the restrictions necessarily imposed by its dimensional form in that the defining constants, slope and intercept, as they appear generally to have been evaluated and reported in the literature, are those strictly appropriate to particular cases and not ones having universal application. For the latter the formulation must take account of the very different physical scales involved with the range of species dealt with and it should account explicitly for variations with time, where this quantity is also expressed in suitable non-dimensional terms. This cannot be done other than approximately with a power law in a formulation of the kind established by Yoda *et al.* (1963). The minus $\frac{3}{2}$ thinning rule has, nevertheless, been widely cited in descriptions of this important growth phase with much attention focused on the values its defining constants should take for the law to become one having universal status. It has also been subsumed in a derivation by Hozumi (1977, 1980) of growth life-lines satisfying logistic laws for biomass production in stands.

The quest for the universality of a power law formulation fundamentally unsuited to its purpose has resulted in many, sometimes conflicting, discussions of the values that should be assigned to its defining constants (see, for example, Gorham 1979; White 1981; Weller 1987; Lonsdale 1990). Most, if not all, of these could have been resolved relatively easily had attention been given to the establishment of suitable non-dimensional forms for the equations used for describing growth in any one of the phases, and also to the composition of the dimensional power laws themselves. This, as will become clear, is because the

PHILOSOPHICAL TRANSACTIONS OF THE ROYAL SOCIETY B BIOLOGICAL SCIENCES
PHILOSOPHICAL TRANSACTIONS OF THE ROYAL SOCIETY B BIOLOGICAL SCIENCES

Downloaded from rstb.royalsocietypublishing.org

non-dimensional forms show which of the quantities and parameters they contain influence growth features, in both form and circumstance, and what effects these have on values that may or may not be assigned to constants of the kind referred to above, given that such constants in fact exist. The use of, for example, the mass per unit area as a principal unit for recording accumulated growth, and of the number of plants per unit area of ground covered for defining planting density, or the equivalent of these dimensional quantities without further qualification, is by no means satisfactory because of the very large range of completely different and unrelated physical scales, different planting patterns, and also different environments, which must be accounted for. The choice of units for recording mass and planting density must be made in such a way that, *inter alia*, between-species differences of height, radius, and canopy shape are taken into account when dealing with mass, and that the selected ground reference areas are areas related to plant dimensions and not ones selected in an arbitrary and perhaps meaningless way. A satisfactory resolution of these problems of dimensions and scaling is of importance for further progress and, because of this, is dealt with early in the present work.

The equations that have been formulated here surmount the problem of physical scale in that they describe the three growth phases in a unified non-dimensional form, which takes account of the physical dimensions and growth times of widely different species. This has been achieved by considering each plant as being enclosed within the otherwise inviolable airspace of a cylinder, just sufficiently large to accommodate it at any one instant in time, and by relating the radiant energy input across the surface of the plant canopy envelope within the cylinder to salient physical features of plant geometry and planting density and pattern on the plane of cultivation. In this description of plant geometry, and also for that of the radiation process, mean values were used. For the plant cylinder, the dimensions assigned to it were those of the statistical mean radius and height for the enclosed plant at each stage of its growth. For the energy conversion process, physical and biological details were omitted in favour of a time-averaged description wherein the diurnal and annual variations of solar energy input at a given global location were replaced, in effect, by what amounts to the solar constant. The non-dimensional units of time used throughout were based on the half-life times for individual species because this quantity is possibly the least difficult and most meaningful one to establish for any case.

The formulae which have been derived are specifically for continuous growth processes in monocultures and, as such, account for the salient features of stand evolution from planting to maturity, at arbitrary packing densities, without obscuring these with details of discrete effects, such as those occurring when individuals are dying off and those due to the mixing of different architectures and light intensities in multicultures. Refinements dealing with these and similar kinds of detail, such as have been considered for the self-thinning process by Aikman & Watkinson (1980), Cannell *et al.* (1984), Perry (1984), Westoby & Howell (1986) and Barreto (1990), for the effects of light on competition by Ford & Diggle (1981), for the effects of interference and hierarchical development by Firbank & Watkinson (1985), for variations in branching patterns by Steingraeber & Waller (1986), and for structural composition taking account of the sort of detail considered by Whittaker & Woodwell (1968), can be made later as and when they are required.

The results obtained indicate that, for given levels of radiation and soil fertility, the biomass growth in Phase I depends only on plant canopy radius, height and shape. In Phase II it becomes additionally dependent on the inverse of the planting density; in Phase III a further alteration takes place to include an inverse dependence on the geometric pattern in which plants are arranged in a stand. The results for Phase III growth do not provide an explicit statement of the minus $\frac{3}{2}$ thinning rule mentioned earlier but it is clear that, for some combinations of plant size, shape and density, the feature is a dominant one for part of the growth process in that, when considered separately from possible variations of thinning-line slope with time, it defines a limiting boundary of greatest negative slope for the entire class of possible thinning lines. When time is taken into account, and the true shape of the thinning line becomes apparent from the growth surfaces showing the variation of biomass and planting density with time, it is equally clear that the minus $\frac{3}{2}$ thinning rule is, at best, only an approximate one.

In more detail, the results show the sort of differences to be expected when assigning values to constants in power laws assumed for approximate descriptions of the self-thinning process, and the sources of these differences in terms of plant canopy dimensions and shape, planting pattern, fertility and radiation. When taken together with the probabilistic diffusion of properties at the lines of demarcation between the growth phases, the effects on individual life-lines followed on the growth surfaces can become quite marked in some cases. These two features alone may explain, at least in part, some of the difficulties of interpretation of measurements of biomass and planting density that have been discussed elsewhere (White 1981; Weller 1987; Lonsdale 1990).

Because each plant cylinder is defined in terms of a statistical mean boundary, which is assumed inviolable, the possible consequences of statistically significant canopy overlap (Gates *et al.* 1979; Firbank & Watkinson 1985) are not considered, and mutual contact between plant cylinders is regarded as a theoretical limit to radial growth. This in no way precludes the presence of canopy overlap and overtopping in a stand, as these clearly exist in any case because of the deviations about the means inherent in defining plant mean radius and height. What the limit implies is that either there is no subsequent radial development, so that plants become deformed, or the number of plant cylinders of a given uniform mean size within the solar cylinder at any one time is reduced by self-thinning, or a hybrid combination of these takes place. What this

PHILOSOPHICAL TRANSACTIONS OF THE ROYAL SOCIETY B BIOLOGICAL SCIENCES
PHILOSOPHICAL TRANSACTIONS OF THE ROYAL SOCIETY B BIOLOGICAL SCIENCES

Downloaded from rstb.royalsocietypublishing.org

amounts to in turn, for otherwise uniform growth and the preservation, or evolution, of a self-preserving optimum geometric pattern on the plane of cultivation, is that thinning may also follow some sort of organized pattern, possibly of the kind indicated qualitatively, and tentatively, in examples of hexagonal, square and non-uniform packing arrangements.

It is also shown by using a quasi-static analysis that, where the thinning process follows the perhaps more usual course of a progressive development of a non-uniform hierarchy, the competition process is one that can be initiated in the early stages of Phase II growth, or in some cases even in Phase I growth, before the accumulation of biomass has reached one half of its possible maximum. For most cases this is well before there is any mutual contact of plant cylinders, let alone any significant overlap or overtopping of canopies. This particular analysis indicates, in some detail, the variation of biomass with time for a binary planting distribution of uniformly augmented and diminished biomass. It shows the consequences of one-sided competition processes favouring the larger sizes, and also circumstances, like those of nearly dead trees, in which recovery to normal or near-normal growth is possible from a temporary stage involving a large residual amount of non-living tissue coexisting with a small, perhaps even minute, portion of living tissue at a given instant. Some of the initial conditions used for the binary distribution were also consistent with the evolution of clumps in stands.

Because plant canopy envelope geometry appears as a component in the expressions for biomass derived for each of the growth phases, there is a need for a suitable preliminary classification of the many possible geometric shapes into groups having fundamental similarities. This has been done so as to include shapes considered elsewhere (Assmann 1970; Gates *et al.* 1979), but is not limited in accord with the restrictions inferred for the upper surface shapes of overlapping crown structures by Gates *et al.* (1979). Eight such groups, comprising five primary and three higher-order compound shapes, each generated as a surface of revolution with a simple mathematical description, are considered adequate for the present purpose. For the primary shapes the required formulae are tabulated in a suitable non-dimensional form, but this has not been done for the higher-order compound ones because of the enormous range of possible geometric combinations within even that relatively simple subclass.

ANALYSIS I: BIOMASS AND PLANTING DENSITY

For idealized growth on a horizontal plane surface, each plant in a uniformly distributed monoculture has, by definition, exactly the same dimensions at a given time and may be assumed enclosed in the inviolable airspace of a cylindrical envelope, of radius R and height H, as shown in figure 1.

The total above-ground surface area S_c through which radiation energy, and all derivatives of this contributing to growth, may pass is the plant gross-

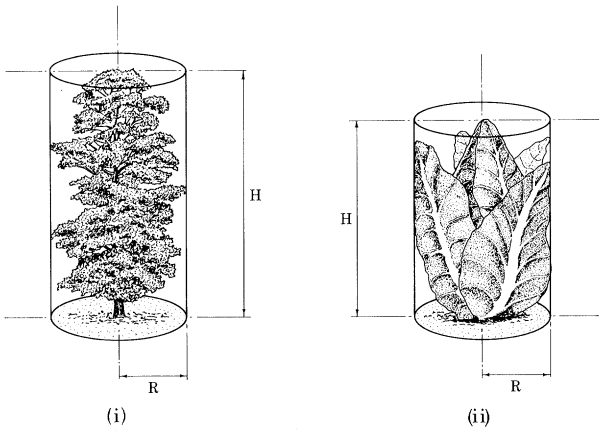

Figure 1. The plant cylinder, with radius R and height H, is shown enclosing (i) a common elm (*Ulmus procera*) and (ii) a spring cabbage (*Brassica oleracea* var.). These are 'ideal' plants conforming in their dimensions to those of the statistical means for the species populations.

radiation or environmental surface defined by

$$S_c = \pi R^2(1+2H/R), \quad (1)$$

and this encloses a volume $V_c = \pi R^2 H$ but does not include the cylinder base at ground level. The dimensions of this plant cylinder, and all subsequent similar and associated ones referred to here, are not measurably exact quantities but statistical means representing the radial and height dimensions of plants in normal healthy species monocultures. Its volume is taken as that available to each plant for the photosynthesis of radiant energy from the environment in producing a total desiccated biomass of amount $M(t)$, with no distinction made between the various means by which this is achieved, or of the various direct and diffuse forms the energy input may take (Monteith 1973).

The actual radiation energy received by the plant is considered as taking place across the surface area S of the canopy envelope within the plant cylinder shown in figure 2. In calculating this area S, account is taken of the reduction with height H_0 above ground of the effectiveness of the flat circular disc of radius R_0, used to represent the canopy undersurface, for the conversion of diffuse and reflected usable radiant energy. This is achieved by expressing the base contribution to S as $K_0 \pi R_0^2$, where $K_0 = 1 - \exp(-k_0 H_0/R)$, and k_0 is a coefficient suitably describing the attenuation of the radiation in this umbratic region. For a canopy undersurface far above ground, K_0 thus takes values near to unity, and for one at ground level K_0 becomes zero, thereby excluding in this case the canopy undersurface in its entirety, as was done for the plant cylinder. Calculation methods and details are dealt with in Appendix 1.

For the population of a uniform stand which is of infinite extent, in the sense that the effects of discontinuities at the stand perimeter may be ignored when dealing with a majority of the members of the otherwise uniform distribution, a suitable solar radiation surface of area S_s may be defined in terms of a solar cylinder, of radius R_∞ and height H, with

$$S_s = \pi R_\infty^2(1+2H/R_\infty). \quad (2)$$

PHILOSOPHICAL TRANSACTIONS OF THE ROYAL SOCIETY B BIOLOGICAL SCIENCES
PHILOSOPHICAL TRANSACTIONS OF THE ROYAL SOCIETY B BIOLOGICAL SCIENCES

Downloaded from rstb.royalsocietypublishing.org

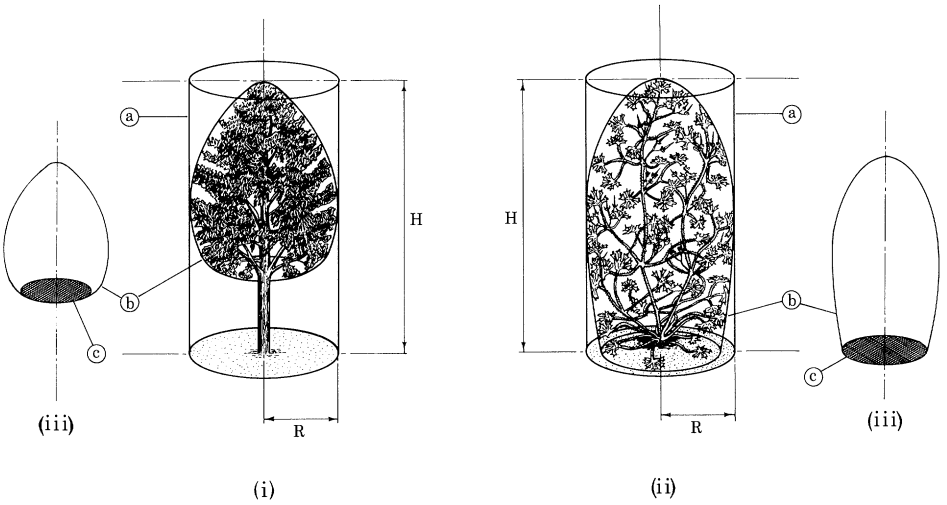

Figure 2. The plant cylinders (a) and canopy envelopes (b) are shown enclosing (i) a cricket-bat willow (*Salix alba* 'Coerulea') and (ii) a 'cut-leaved cranesbill' (*Geranium dissectum* L.). Both are 'ideal' plants (see caption to figure 1). The canopy envelopes (b) are shown to reduced scales at (iii) with the flat circular discs of their undersurfaces (c) cross-hatched.

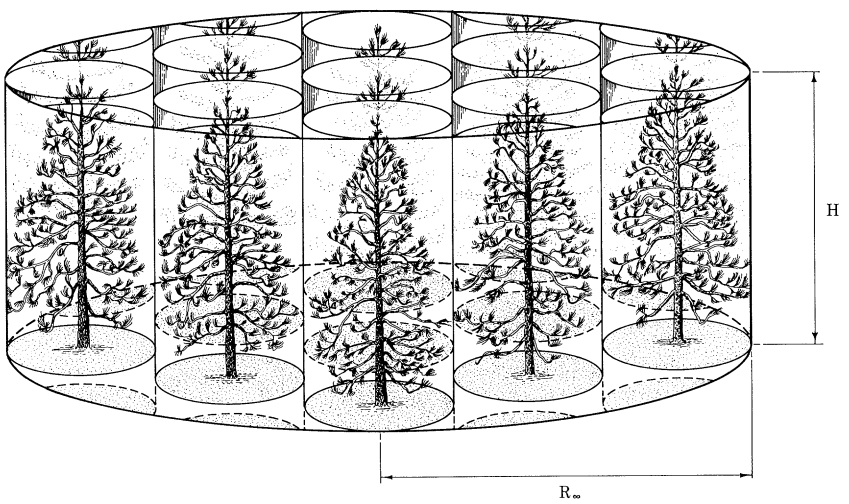

Figure 3. The solar cylinder of fixed radius R_∞ and variable height H is shown enclosing, in whole and in part, a uniformly distributed number of identical 'ideal' (see caption to figure 1) plant cylinders each of radius R and height H. At the final stage of growth, when self-thinning is complete, only one plant cylinder will exist and this will fill completely the solar cylinder of radius R_∞ and ultimate height H_∞.

Initially, this solar cylinder includes, in whole and in part, a number of plant cylinders within its boundaries. When growth is complete the height H and surface area S_s of the solar cylinder attain their maximum values H_∞ and S_∞. In these circumstances the solar cylinder has just enough room to accommodate one fully grown plant, also of height $H = H_\infty$ and radius R_∞, in isolation at a given packing density, and such that the interception of usable radiation, and also the fertility and nutrient levels, are perfect for this amount of growth. The arrangement is shown in figure 3.

Each solar cylinder receives radiant flux at its boundary surfaces, which do not include the base of the cylinder. If $\phi_s(t)$ is the radiant energy flux received on S_s at time t and effectively contributing to biomass production, then this is supposed sufficient to produce an effective mean biomass density within the solar cylinder of amount $F(t)\rho_s$, where $F(t)$ is a function representing the fertility and nutrient availability level at the place of planting, and ρ_s is the actual mean biomass density that could be produced in the volume V_s, enclosed by S_s under perfect fertility and nutrient supply conditions, where $F(t)$ has its upper bound value of unity. $F(t)$ has a lower bound of zero defining either or both complete infertility and zero nutrient level.

The corresponding radiant fluxes and effective biomass densities on and within the plant cylinder and canopy envelope are $\phi_c(t)$, $\phi(t)$, $F(t)\rho_c$ and $F(t)\rho$, respectively. The radiant flux $\phi(t)$ is a fraction of that available for conversion and the ratio $\phi(t)/\phi_c(t)$ is a measure of the efficiency with which the conversion of radiant energy to biomass is accomplished by different species. For equal mean values of irradiance on the plant cylinder and canopy envelope surfaces the ratio $\phi(t)/\phi_c(t)$ is therefore taken to be such that

$$\phi/\phi_c = S/S_c = \rho/\rho_c, \qquad (3)$$

Downloaded from rstb.royalsocietypublishing.org

and the total biomass $M(t)$ produced in the canopy volume V enclosed by the canopy surface of area S is of amount

$$M(t) = F(t)\,\rho V = F(t)\,\rho_c(S/S_c) \times V = \pi F(t)\,\rho_c\,\Lambda(t)\,\{R(t)\}^2\,H(t), \quad (4)$$

where $\Lambda(t) = (S/S_c)\,(V/V_c)$ is a canopy shape parameter. This parameter can be used to distinguish classes of plants, of otherwise similar or dissimilar species, in terms of the amount of radiation envelope surface and volume, relative to those of the plant cylinder, that each class requires for biomass production. Methods for evaluating the shape parameter are given in Appendix 1.

The biomass densities ρ, ρ_c and ρ_s are relative and not absolute. They are used with the volumes enclosed within the surfaces S, S_c and S_s to evaluate respectively, the total actual biomass M of the plant, the total biomass M_c that could be produced within the plant cylinder, and the total biomass M_s produced within the solar cylinder at time t. Equation (4) shows that biomass production is greatest when S becomes as close as is possible to its upper limiting value S_c, and the waste of available radiant energy is least.

At any instant during growth the number of plants within the radius of the solar cylinder is X, so that the total assembly of plant gross radiation surfaces has area of amount XS_c. It is in comparing this area with that of the solar cylinder that possible reasons for the three distinct phases of growth become apparent. Such a comparison also leads naturally to the selection of the area of an end face of the solar cylinder as the reference one appropriate for defining planting density, for by this means the full growth unit of planting density is always unity, and intermediate values related multiples of this, for all species.

For Phase I, $XS_c \leqslant S_s$, and as long as the inequality is satisfied there is an excess of radiant energy and physical space available to each plant. In these conditions growth is wholly unrestricted and commensurate with the supply of nutrients until the phase boundary, defined by $XS_c = S_s$, is reached. On this boundary X takes the value X_p, where

$$X_p = (1/\lambda_r)\,(\lambda_\infty + 2\lambda_h)/(\lambda_\infty\lambda_r + 2\lambda_h), \quad (5)$$

where $\lambda_r = R/R_\infty$, $\lambda_h = H/H_\infty$, $\lambda_\infty = R_\infty/H_\infty$, and the sum of the areas of all of the plant cylinders becomes equal to that of the solar cylinder. λ_∞ is the plant slenderness ratio. In Phase I, $\rho_c = \rho_s$ and (4) becomes

$$\mu_1 = \lambda_r^2\,\lambda_h, \quad (6)$$

where $\mu_1 = M(X,t)/(M_\infty\,\sigma\Lambda)$, $M_\infty = \pi F(t)\,\rho_\infty R_\infty^2 H_\infty$, and $\sigma = \rho_s/\rho_\infty$ is the biomass density ratio assumed constant for a given canopy and environment. In these statements M_∞ is the ideal total mean biomass that could be produced in a solar cylinder of height $H = H_\infty$ under conditions where the received usable radiation is totally adequate for full and complete mean growth with corresponding biomass density ρ_∞. The ratio σ of the actual to ideal mean biomass densities describes, in its effect, the extent to which the actual radiation environment differs from the ideal one. In normal circumstances $\sigma = 1$, but for locations offering augmented or diminished radiation levels, by natural or artificial means, then σ is accordingly greater or less than unity respectively.

Equations (5) and (6) are in a unified non-dimensional form which is suitable for direct comparisons of fundamental growth properties irrespective of the physical size, shape and radiation environment of different kinds of plants, and also of their growth time because of the dependence of biomass production on this quantity. In particular, (6) is a non-dimensional statement of plant cylinder volume at time t. Such forms will be used subsequently in all cases except for those requiring an explicit dimensional presentation.

For Phase II, $XS_c > S_s$, and although none of the plant cylinders is yet touching any other one, the gross radiation surface of each now exceeds that available to it in an equable division of radiation resources in the solar cylinder. In such competitive conditions normal biomass production rates cannot be maintained and the consequent self-regulation of growth in accord with energy conservation may engender a plastic response in which either, or both, the limbs of individual plants in otherwise uniform stand growth subsequent to the plastic line (5) become different from normal, or the stand growth itself becomes non-uniform. In Phase II, $\rho_c \neq \rho_s$, and the biomass density is now specified using the conservation equation

$$X\rho_c S_c = \rho_s S_s, \quad (7)$$

which defines an equable distribution of radiant energy among the plants within the solar cylinder. In this case (4) becomes

$$\mu_2 = (\mu_1/X)\,(\lambda_\infty + 2\lambda_h)/[\lambda_r(\lambda_\infty\lambda_r + 2\lambda_h)]. \quad (8)$$

Phase III growth takes place when $XS_c > S_s$ and the plant cylinders actually begin touching. This phase is taken here to be a limiting one in the sense that no further radial growth is considered possible unless the number of plant cylinders within the solar cylinder is reduced. In this respect it is important to note that, because each plant cylinder has the dimensions of the mean radius and height appropriate to a particular stage of growth, there will always be canopy overlap and overtopping present in any case within a stand having a logarithmic-normal distribution of plant sizes (Koyama & Kira 1956), or, for that matter, any other type of distribution, with finite variance.

The auto-regulatory self-thinning process by which means such a reduction in the number of plant cylinders present at any one time is achieved is thus an axiomatic consequence of plant cylinder inviolability and much, if not most, of the relevant detail describing it follows at once. Other details which may be associated with the self-thinning process, such as those attributed to canopy overlap (Gates *et al.* 1979; Firbank & Watkinson 1985), and those arising from the effects of non-uniform growth and overtopping by neighbours (Ford & Diggle 1981), are not considered here.

In this limiting phase the arrangement of the plant cylinders on the plane of cultivation within the solar cylinder defines how much of the already reduced amount of radiant energy is available to each plant

PHILOSOPHICAL TRANSACTIONS OF THE ROYAL SOCIETY B BIOLOGICAL SCIENCES
PHILOSOPHICAL TRANSACTIONS OF THE ROYAL SOCIETY B BIOLOGICAL SCIENCES

Downloaded from rstb.royalsocietypublishing.org

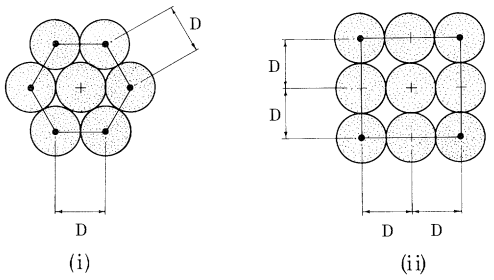

Figure 4. Two kinds of uniform packing arrangements for plant cylinders in mutual contact: (i) close-packed hexagonal; (ii) close-packed square.

from the overall distribution. Figure 4 shows two types of packing for a uniform distribution of plant cylinders with centres at separation distances $D = 2R$ on a plane surface. The plane spatial efficiency of arrangements like these may be expressed in terms of a packing coefficient C_p defined as the ratio of the area covered by each cylinder to the total area available to it (Stephenson, 1971). For infinite and uniform arrays the packing coefficient $C_p = \frac{1}{6}\pi\sqrt{3}$ for the hexagonal arrangement and $C_p = \frac{1}{4}\pi$ for the less-dense square distribution. For finite arrays within the solar cylinder the value of the packing coefficient C_p for the region within it changes as the number of plants becomes reduced by self-thinning and methods for evaluating it are given in Appendix 2.

For plant cylinders in mutual contact it follows that the planting density X must satisfy

$$X = X_t = C_p/\lambda_r^2 \tag{9}$$

for the continued normal growth of individuals at reduced rates and, with the biomass density again defined by (7), (4) now takes one of the equivalent limiting forms

$$\mu_3 = (\lambda_h/X_t)(\lambda_\infty + 2\lambda_h)/[\lambda_\infty + 2\lambda_h(X_t/C_p)^{\frac{1}{2}}]$$
$$\text{or} \quad \mu_3 = (\mu_1\lambda_r/C_p)\,[(\lambda_\infty + 2\lambda_h)/(\lambda_\infty\lambda_r + 2\lambda_h)], \tag{10}$$

for growth on the self-thinning line. It is clear from (10) and the constraint condition (9) that the self-thinning line is not an asymptote of (8), except when $C_p = 1$ everywhere, and that in the growth process the plastic line is encountered before the thinning-line as long as

$$2(\lambda_h/\lambda_r)\,(C_p - \lambda_r)/(1 - C_p) > \lambda_\infty. \tag{11}$$

Several points of detail are now immediately obvious. First, for a given geometric shape $A(t)$ and density ratio σ, (6) is independent of planting density, (8) is inversely proportional to this quantity, and (10) has a two-component inverse dependence on it. The X dependence for (6) and (8) is the same as that quoted elsewhere (see, for example, White, 1981), but that in (10) does not conform directly to a $-\frac{3}{2}$ thinning rule. It is clear that, in (10), when

$$2(\lambda_h/\lambda_\infty)\,(X_t/C_p)^{\frac{1}{2}} \ll 1, \tag{12}$$

then, for a given λ_h, μ_3 behaves asymptotically as X_t^{-1}, and when the second-order inequality is reversed, the asymptotic behaviour is as $X_t^{-\frac{3}{2}}$. The first of these conditions can arise with dominantly radial growth at low planting density, for which λ_∞ is large and X_t is small (for example, when $\lambda_h/\lambda_\infty \to 0$). The second condition is favoured by plants that are ultimately tall and slender, for which λ_∞ is small, at growth stages where both λ_h and X_t are large (when $\lambda_\infty \to 0$ then $\mu_3 = \sqrt{(C_p)/(2X_t^{\frac{3}{2}})}$). Equation (10) therefore amounts approximately to a $-\frac{3}{2}$ thinning rule only when this second condition is satisfied. There is otherwise a direct and significant involvement of plant geometry and height leading to a hybrid dependence on both X_t^{-1} and $X_t^{-\frac{3}{2}}$ during growth. In conditions of abnormal growth the interdependence of different from normal radial and height dimensions, λ_r and λ_h, and planting density X, may lead to even less clear indications of the progress in the energy-biomass conversion process of a community. To deal with these, the departures from normality would have to be specified for each case.

Secondly, the dependence of (10) on the packing coefficient C_p is not one that is very sensitive to the small changes that are evident in this quantity for numbers X_t greater than about 12 (see Appendix 2). Because of this C_p was assigned constant values for planting densities in excess of 12 in subsequent calculations made by using (10), for both close-packed hexagonal ($C_p = \frac{1}{6}\pi\sqrt{3}$ and square-packings ($C = \frac{1}{4}\pi$).

Thirdly, as plants die off the corresponding discrete changes that take place in the packing coefficients will depend on whether the thinning process itself is either one of self-preservation of an already optimum pattern, one of evolution from a less-efficiently packed arrangement towards an optimum, or one that remains haphazard. This question is discussed tentatively later.

Fourthly, the two limiting cases $\lambda_\infty \to 0$ and $\lambda_\infty \to \infty$, which between them distinguish hypothetical extremes of plant geometry, reduce (8) and (10) to the forms

$$\lim_{\lambda_\infty \to 0} X_p = 1/\lambda_r, \quad \lim_{\lambda_\infty \to 0} X_t = C_p/\lambda_r^2, \tag{13}$$

which together imply that $X_p \leqslant X_t$ for $\lambda_r \leqslant C_p$, and

$$\lim_{\lambda_\infty \to \infty} X_p = 1/\lambda_r^2, \quad \lim_{\lambda_\infty \to \infty} X_t = C_p/\lambda_r^2, \tag{14}$$

which mean that $X_t \leqslant X_p$ for $C_p \leqslant 1$. The limits (13) amount to a description of plants with radial growth but no height ($\lambda_h \to 0$), whereas (14) is for plants having height but no radius ($\lambda_r \to 0$). Real plants satisfy conditions between these two limits, which are significant in that they show the importance of efficient packing on the plane of cultivation if unnecessary self-thinning is to be avoided.

Fifthly, it is clear that, for a given initial planting density and growth with time, the life-lines are unique if, and only if, the parameters λ_h, λ_r, λ_∞ and C_p are the same for all values of time. This result is partly in accord with the observations of Weller (1987).

Lastly, it is important to note that, although all of the above results involve only salient features of plant canopy geometry in relation to the space which can be occupied by each plant cylinder, they are, nevertheless, sufficient for an initial resolution of at least some of the questions that have been raised in the literature about the three growth phases, and, in particular, about the self-thinning rule (White 1981; Hutchings 1983;

PHILOSOPHICAL TRANSACTIONS OF THE ROYAL SOCIETY B BIOLOGICAL SCIENCES
PHILOSOPHICAL TRANSACTIONS OF THE ROYAL SOCIETY B BIOLOGICAL SCIENCES

Downloaded from rstb.royalsocietypublishing.org

Weller 1987; Lonsdale 1990). These matters are dealt with later in the discussion.

ANALYSIS II: THE GROWTH SURFACE

In normal, natural growth, $\mu_{1,2,3}$, λ_r and λ_h are mutually dependent functions of time and when these functions are defined the surface containing the growth life-lines can be constructed. On this surface the plastic and thinning lines define the growth-phase boundaries. In most cases the growth life-line will cross the plastic line, once, and once only, thereafter proceeding towards the self-thinning line. The latter is strictly a one-sided limit to growth only when the variances of the means $M(t, X)$ and $X(t)$ are zero, and this is unlikely in all real cases. It is otherwise an approximate two-sided limit in the sense that the growth life-line may tend, in some cases, to overshoot slightly in its approach to the self-thinning line.

Within the solar cylinder the overall accumulation of biomass resulting from the input of radiant energy is distributed in different ways according to which of the growth phases exists at a particular instant. Different species have different natural life-time scales and, if between species comparisons are to be made, it is necessary to replace these natural time-scales by a non-dimensional one. This can be achieved by taking

$$\tau = t/t_{\frac{1}{2}}, \tag{15}$$

where $t_{\frac{1}{2}}$ is the half-life time for normal, natural growth, defined by

$$M/(M_\infty \sigma \Lambda) = \tfrac{1}{2}, \tag{16}$$

and where there is no present need to retain the suffix 1 of (6). For many cases of interest, the half-life time $t_{\frac{1}{2}}$ will occur more or less in conjunction with the larger rates of biomass production in the growth cycle and is, therefore, likely to be much more sharply defined than other possible reference times, such as the total lifetime t_∞. It is also a quantity that should not prove difficult to establish statistically for individual species.

Before establishing general and particular forms of the growth surface it is of considerable importance to give consideration to the differential equations describing biomass production rates within the solar cylinder. This is because these rates exert a controlling influence on the dynamics of the growth process as a whole and also define the circumstances in which biomass accumulation instabilities can lead to one-sided competition. For normal, natural growth, the differential equation

$$\mathrm{d}\mu/\mathrm{d}\tau = \beta\mu^p(1-\mu^{q-p}), \quad \beta > 0, \tag{17}$$

which is a generalized, non-dimensional form of the equation devised by von Bertalanffy (1941, 1957), defines a class of growth equations restricted analytically only by their integrability. In particular, and for integer exponents, the immediately recoverable solutions are for the exponential $(p = 1, q = -\infty)$, monomolecular $(p = 0, q = 1)$ and autocatalytic $(p = 1, q = 2)$, growth forms (Medawar 1945; Richards 1959; Steward, 1968; Hunt, 1982). The Gompertz (1825) growth form satisfies the differential equation

$$\mathrm{d}\mu/\mathrm{d}\tau = -\beta\mu \ln(\mu), \tag{18}$$

and this can be obtained from (17) by replacing β with $\beta/(q-p)$ and then proceeding to the limit $q \to p$ to obtain,

$$\mathrm{d}\mu/\mathrm{d}\tau = -\beta\mu^p \ln(\mu), \tag{19}$$

in general, and (18) in particular when $p = 1$, as indicated by Richards (1959). The Gompertz form (18) behaves like the autocatalytic one as μ approaches unity.

An important feature of the differential equation (17) is the dynamic response with time τ to a small perturbation $\delta\mu$ in the mass μ. It is not difficult to show from (17) that this is

$$\begin{aligned}\frac{\mathrm{d}}{\mathrm{d}\tau}(\delta\mu) &= \beta(p\mu^p - q\mu^q)(\delta\mu/\mu) \\ &\quad + [p(p-1)\mu^p + (p-q) \\ &\quad \times \{2p(p-1) - q(2p-1)\}\mu^q](\delta\mu/\mu)^2/2 + \ldots. \end{aligned} \tag{20}$$

On retaining only the terms to first order in $\delta\mu$, as is customary in an analysis of this kind, it follows that there is a subsequent decay of this quantity with time, $\mathrm{d}(\delta\mu)/\mathrm{d}\tau < 0$, if

$$\beta(p\mu^p - q\mu^q) < 0, \quad \beta > 0, \tag{21}$$

and, except for the Gompertz form, this means that

$$q > p\mu^{p-q}, \quad \mu \in [0, 1]. \tag{22}$$

Exponential growth $(p = 1, q = -\infty)$ is therefore unstable for all values of μ, as is intuitively obvious; the monomolecular and Gompertz growth forms are stable for all values of μ; and the autocatalytic form is unstable for $\mu < \frac{1}{2}$ and stable for $\mu > \frac{1}{2}$, for which $\tau < 1$ and $\tau > 1$ respectively. What this means is that plants in autocatalytic growth, which have not yet attained one half of their ultimate normal mean mass, and which have acquired by some means a slightly larger mass $(\mu + \delta\mu)$ than neighbouring ones having mass μ in an environment of adequate radiation, will begin progressively to outgrow their neighbours and establish a one-sided competition process. At later times, when the mass differences become finite, the whole process is likely to become accelerated by overtopping and the effect this has in reducing the density ratio σ for shorter neighbours in greater shade. The degree of non-uniformity it causes will be greatest when the packing is at its most dense because the diffusion of locally augmented shading with distance from the umbratic source means that near neighbours being overtopped are placed at a much greater disadvantage than more distant ones. In this respect, overtopping and the alterations engendered by it in the competition for radiation are consequences, but not causes, of the destabilization process.

Of the possible solutions of (17), the class defined by

$$\mu = \lambda_r^2 \lambda_h = \{1 + \alpha_m \exp(-\beta_m \tau)\}^{\gamma_m}, \tag{23}$$

following Richards (1959), permits the immediate recovery of the monomolecular $(\gamma_m = 1)$ and auto-

PHILOSOPHICAL TRANSACTIONS OF THE ROYAL SOCIETY B BIOLOGICAL SCIENCES
PHILOSOPHICAL TRANSACTIONS OF THE ROYAL SOCIETY B BIOLOGICAL SCIENCES

Downloaded from rstb.royalsocietypublishing.org

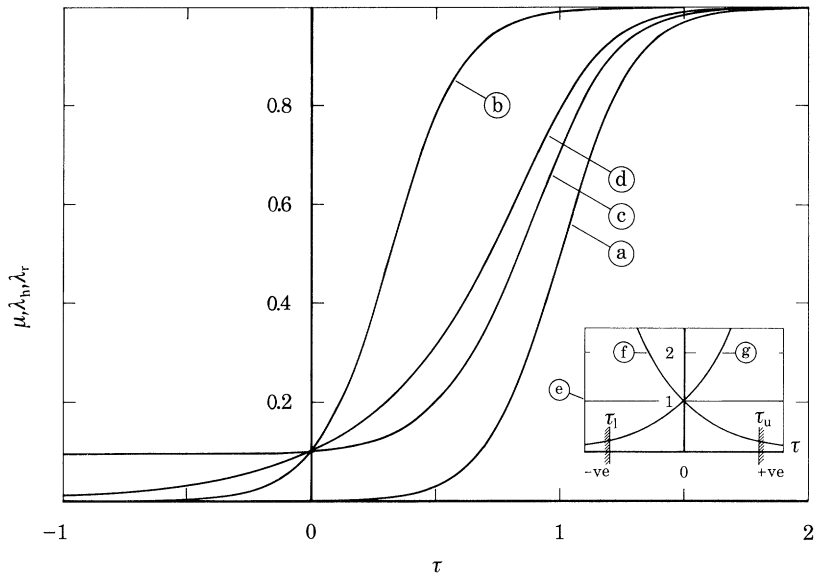

Figure 5. Example growth curves and limit boundaries (inset). Curves (a), (b) and (c) are for autocatalytic growth for which $\mu_0 = 0.001$, $\lambda_{h0} = 0.1$, $\alpha_m = 999$, $\alpha_h = 9$, $\beta_m = 6.906\,755 = \beta_h$, $\lambda_\infty = 1$. (a) Non-dimensional mass μ. (b) Non-dimensional height λ_h. (c) Non-dimensional radius λ_r. Curve (d) shows the variation of $\lambda_r = \lambda_h$ for autocatalytic growth with geometric similarity and values of parameters as above, except for $\alpha_m = 999 = \alpha_h$. The inset figure shows curves of $\exp[(\beta_h - \beta_m)\tau]$ for three values of β_h and β_m. For (e), $\beta_h = \beta_m$ and $0 \leqslant (\alpha_h/\alpha_m) \leqslant 1$. For (f) the upper limiting value for τ is τ_u; the corresponding lower limiting value for curve (g) is τ_l.

catalytic ($\gamma_m = -1$) forms. The differential equations for both of these are, from (17),

$$d\mu/d\tau = \beta(1-\mu) \quad \text{and} \quad d\mu/d\tau = \beta\mu(1-\mu), \tag{24}$$

respectively. The physical interpretation of these equations is that the former states that the mass growth rate is proportional to the amount of biomass yet to be formed for complete growth, whereas the latter defines growth rates which, initially, are proportional to the existing mass and, ultimately, are proportional to the outstanding mass in the growth process. Because the autocatalytic form is arguably the more plausible of these two descriptions, it is the one used here, together with the initial ($\tau = 0$) and maximum growth rate ($\tau = 1$) conditions,

$$\tau = 0, \quad \mu(0) = \mu_0, \quad \lambda_h = \lambda_{ho}; \quad \tau = 1, \quad \mu(1) = \tfrac{1}{2}. \tag{25}$$

The constants α_m and β_m are

$$\alpha_m = (\mu_0)^{1/\gamma_m} - 1, \quad \beta_m = \ln(\alpha_m), \tag{26}$$

and, with $\gamma_m = -1$, (23) simplifies to

$$\mu = 1/(1+\alpha_m^{1-\tau}). \tag{27}$$

The corresponding height growth λ_h is taken to be

$$\lambda_h = \{1 + \alpha_h \exp(-\beta_h \tau)\}^{\gamma_h}, \tag{28}$$

with $\gamma_h = -1$ for the autocatalytic case, and $\gamma_h = -\frac{1}{3}$ for growth in which geometric similarity ($\lambda_r = \lambda_h$) is preserved. The constant α_h takes the value

$$\alpha_h = (\lambda_{h0})^{1/\gamma_h} - 1, \tag{29}$$

leaving β_h to be specified. From (23), the radial growth λ_r must satisfy

$$\lambda_r = (\mu/\lambda_h)^{\frac{1}{2}}, \tag{30}$$

and because $\lambda_r \leqslant 1$, it also follows from (23) and (27) that, for $\gamma_h = -1$,

$$\alpha_h/\alpha_m \leqslant \exp\{(\beta_h - \beta_m)\tau\}. \tag{31}$$

This inequation is always satisfied for $\tau > 0$ if $\alpha_h \leqslant \alpha_m$ and $\beta_h \geqslant \beta_m$. In particular, if $\beta_h = \beta_m$ then (α_h/α_m) can take any value between 0 and 1 and there is no limit for τ. Otherwise there are upper and lower limit boundaries for τ defined by

$$\tau_u, \tau_l = \{1/(\beta_h - \beta_m)\} \ln(\alpha_h/\alpha_m), \tag{32}$$

with the upper limit τ_u occurring when $\beta_h < \beta_m$, and the lower one τ_l when $\beta_h > \beta_m$. Example growth curves and limit boundaries are shown in figure 5.

Equations (5), (6), (8)–(11), (15) and (23) define the autocatalytic growth surface for prescribed initial conditions $\mu = \mu_0$ and $\lambda_h = \lambda_{h0}$, together with specified values of the parameter β_h. Such a surface, together with projections of example plastic, self-thinning and growth life-lines on to the three mutually orthogonal coordinate planes for the possible variable pairs, is shown sketched in figure 6. As it is one or other of these projections that has normally been discussed in the literature, rather than the complete growth surface, particular attention should be given to them in relation to the very different shapes of the curves from which they are derived. It should be noted that the number X of plants at any position on the plastic line (equation 5) is independent of the packing arrangement, and that the corresponding number on the self-thinning line (equation 9) depends only on the relative radius λ_r and the packing coefficient C_p. The plastic and self-thinning lines intersect when $X_p = X_t$, which is when τ is determined, so that the equation

$$\lambda_r(\lambda_\infty + 2\lambda_h) = C_p(\lambda_r\lambda_\infty + 2\lambda_h), \tag{33}$$

PHILOSOPHICAL TRANSACTIONS OF THE ROYAL SOCIETY B BIOLOGICAL SCIENCES
PHILOSOPHICAL TRANSACTIONS OF THE ROYAL SOCIETY B BIOLOGICAL SCIENCES

Downloaded from rstb.royalsocietypublishing.org

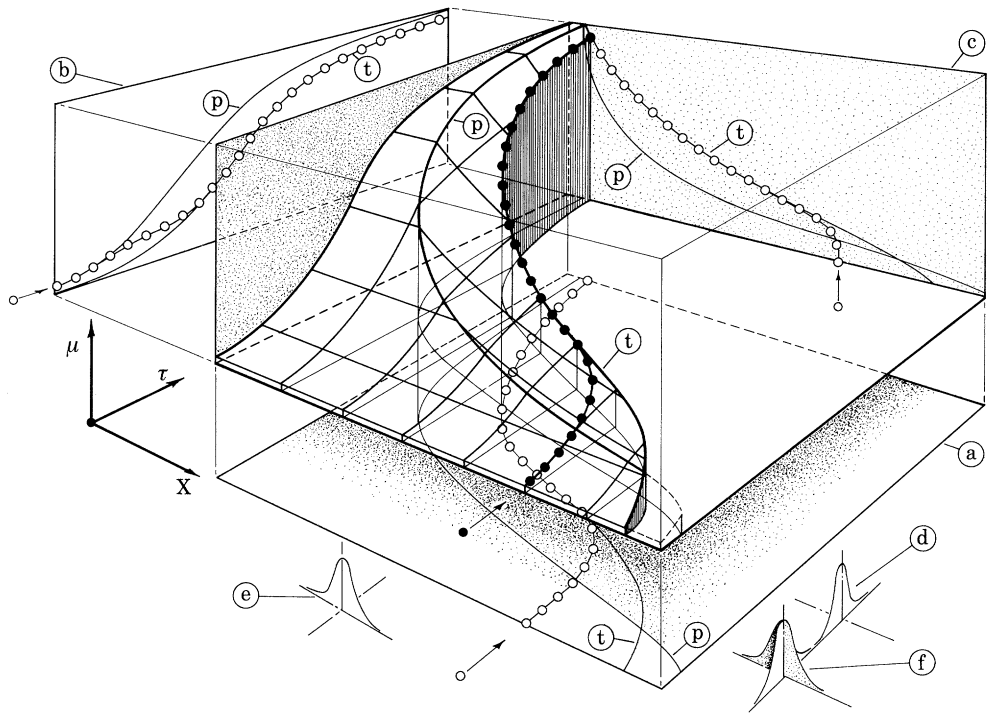

Figure 6. The growth surface showing the variation of non-dimensional mass μ with planting density X and time τ. The surface contours are indicated in the usual way by lines corresponding to constant X and constant τ. The surface is that of a prism for all values of X between 1 and the plastic line (p) which, together with the self-thinning line (t), are shown with their projections on to (a) the τ–X plane, (b) the μ–τ plane and (c) the μ–X plane. The filled circles represent points on a typical growth life-line and the open circles show the projections of this on to the three mutually orthogonal coordinate planes; (d) represents the monovariate Gaussian uncertainty of position on the life-line in the τ–X plane and on the self-thinning line; (e) represents the monovariate Gaussian uncertainty associated with planting density X; (f) represents the bivariate Gaussian uncertainty associated with the mass $\mu(\tau, X)$.

formed from (5) and (9), is satisfied. For initial planting densities $X = X_0$ in excess of this number, only the self-thinning line will be encountered during growth.

When the plastic line is encountered first on the life-line, the subsequent growth up to the self-thinning line is of reduced normal form, with plastic deformation of limbs contributing generally to the preservation of architectural geometry. When the self-thinning line is encountered first, growth becomes subject to alterations such that individuals may have either diminished, normal or augmented biomass, depending on the slenderness ratio λ_∞ and the packing coefficient C_p for the stand. These three cases are distinguished according as the ratio

$$\mu_3/\mu_1 = (\lambda_r/C_p)\{(\lambda_\infty + 2\lambda_h)/(\lambda_\infty \lambda_r + 2\lambda_h)\}, \quad (34)$$

for which the two limits corresponding to the possible extremes of plant slenderness ratio, λ_∞, are

$$\lim_{\lambda_\infty \to 0} (\mu_3/\mu_1) = \lambda_r/C_p \quad \text{and} \quad \lim_{\lambda_\infty \to \infty} (\mu_3/\mu_1) = 1/C_p, \quad (35)$$

obtained from (6) and (10), is less than, equal to, or greater than unity. Except for $t \to \infty$, this condition is always satisfied by the second of the results (35). In other circumstances it is satisfied because the available space is not filled when plant cylinders are in mutual contact and Phase III growth begins with an excess of usable radiant energy available for conversion to biomass. As long as this excess of energy can be taken up then it becomes possible for a larger-than-normal amount of biomass to be produced when self-thinning is taking place in otherwise uniform growth in a stand.

When growth proceeds with complete geometric similarity, such that $\lambda_r = \lambda_h$ for all τ, then

$$R/H = \lambda_\infty = \text{const}, \quad (36)$$

and (6) and (8) become

$$\mu_1 = \lambda_h^3 \quad (37)$$

and

$$\mu_2 = (\lambda_h/X)(\lambda_\infty + 2\lambda_h)/(\lambda_\infty + 2), \quad (38)$$

with $X = X_t = C_p/\lambda_r^2 = C_p/\lambda_h^2$ on the self-thinning boundary.

The demarcation between Phases I and II occurs when

$$X = X_p = (\lambda_\infty + 2\lambda_h)/\{\lambda_h^2(\lambda_\infty + 2)\}. \quad (39)$$

Intersection of the plastic and self-thinning lines in this special case is when

$$C_p(\lambda_\infty + 2) = (\lambda_\infty + 2\lambda_h). \quad (40)$$

The analytical implication of equations (36)–(39) corresponds to that of the earlier work by Yoda *et al.* (1963), in that a single characteristic linear dimension is involved in relating biomass to plant geometry.

Figure 7 shows some calculated results for an autocatalytic growth surface shown as projections onto the three mutually orthogonal coordinate planes

Downloaded from rstb.royalsocietypublishing.org

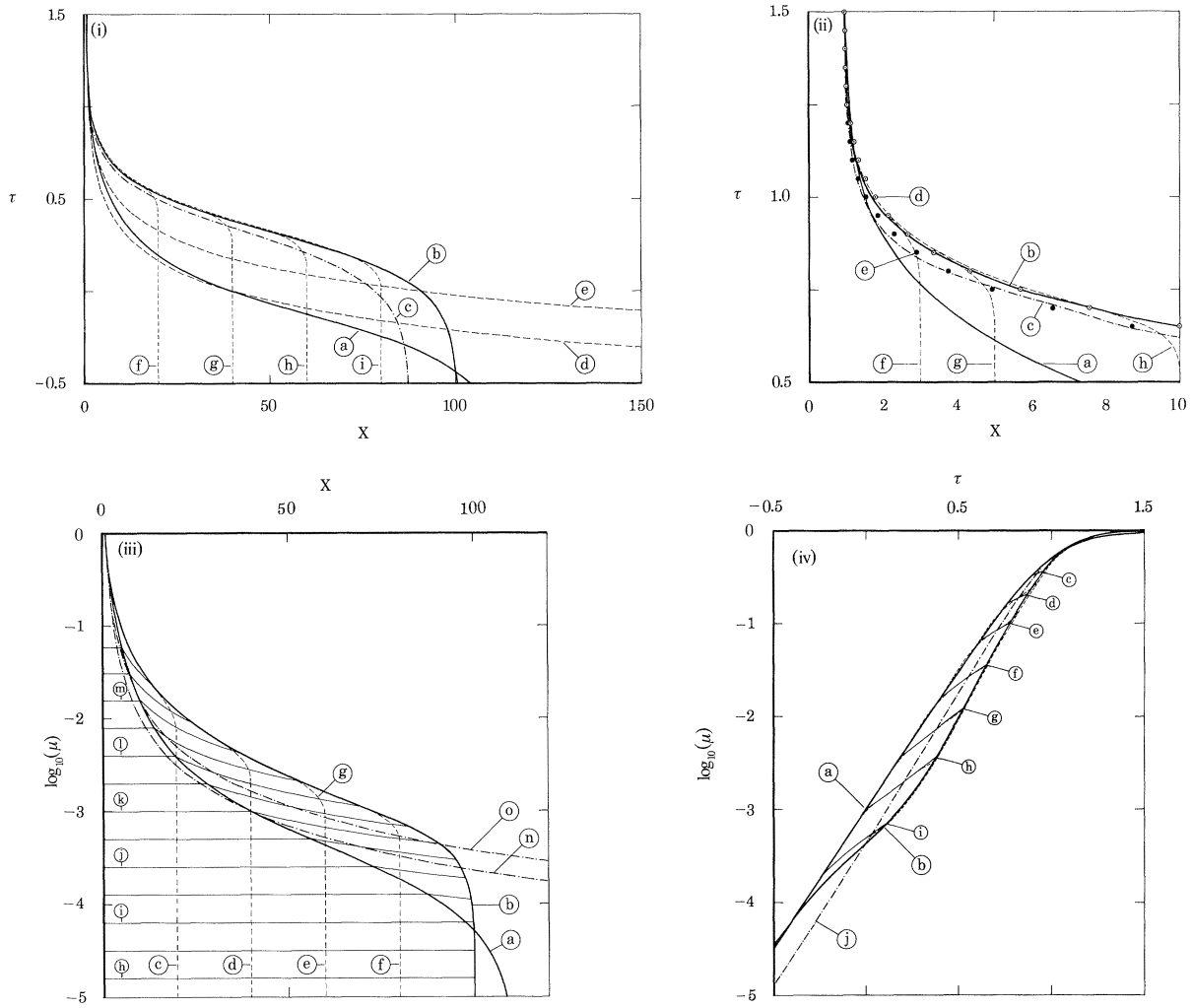

Figure 7. Components of the growth surface calculated for autocatalytic growth with parameter values $\mu_0 = 0.0001$, $\lambda_{h0} = 0.1$, $\alpha_m = 999$, $\alpha_h = 9$, $\beta_m = 6.9067548 = \beta_h$, $\lambda_\infty = 1.0$. The results are for hexagonal packing unless otherwise indicated.

(i) The τ–X plane. (a) The plastic line for both hexagonal and square packing. (b) The self-thinning line for hexagonal packing. (c) The self-thinning line for square packing. (d) The plastic line for growth with geometric similarity, $\lambda_r = \lambda_h$, and parameters as above, except for $\alpha_m = 999 = \alpha_h$. (e) The self-thinning line for growth with geometric similarity. (f–i) Growth life-lines for the following initial planting densities $X = X_0$. (f) 20, (g) 40, (h) 60, (i) 80. These life-lines show the rounding on approach to the self-thinning line and the subsequent slight overshoot of this line resulting from the statistical analysis dealt with later.

(ii) Enlargement of detail, for small values of planting density X to indicate the comparative significance of variations in the packing coefficients C_p with X. (a) The plastic line. (b) The self-thinning line; hexagonal packing. (c) The self-thinning line; square packing. (d) The points within open circles are values calculated with C_p = constant $= (\pi\sqrt{3})/6$. (e) The filled circles are values calculated with C_p = constant $= \pi/4$. (f–h) are growth life-lines as for figure 11 (i).

(iii) The $\mu \sim X$ plane. Logarithms to base 10 have been used for the mass because of the wide range of values dealt with. (a) The plastic line. (b) The self-thinning line. (c–f) Growth life-lines for initial planting densities X_0 as follows: (c) 20, (d) 40, (e) 60, (f) 80. The rounding and smoothing of these life-lines at the growth phase boundaries should be noted. (h–m) Lines on which τ takes the following constant values: (h) −0.6, (i) −0.4, (j) −0.2, (k) 0, (l) 0.2, (m) 0.4. (n) The plastic line; growth with geometric similarity. (o) The self-thinning line; growth with geometric similarity.

(iv) The $\mu \sim \tau$ plane. (a) The plastic line. In this projection the plastic line is coincident with the curve for unrestricted normal growth (see figure 6) because of the prismatic form of this surface in the direction of the X-axis between $X = 1$ and the plastic line. (b) The self-thinning line. (c–i) Growth life-lines for initial planting densities X_0 as follows: (c) 2, (d) 3, (e) 5, (f) 10, (g) 20, (h) 40, (i) 80. (j) The self-thinning line; growth with geometric similarity.

On this figure, the regions where the mass under self-thinning conditions apparently exceeds that for normal natural growth should be noted.

mentioned earlier. The calculations are for the selected values of the parameters μ_0, λ_{h0}, α_m, α_h, β_m, β_h and λ_∞ indicated in the caption to the figure. Figure 8 shows the effects of varying λ_∞ between the two extremes $\lambda_\infty = 10^{-6}$ and $\lambda_\infty = 10^6$ for a given growth function and corresponding growth rates for λ_h and μ. The figure shows that the position of the thinning line is fixed on the $X \sim \tau$ plane, but that of the plastic line varies with

Downloaded from rstb.royalsocietypublishing.org

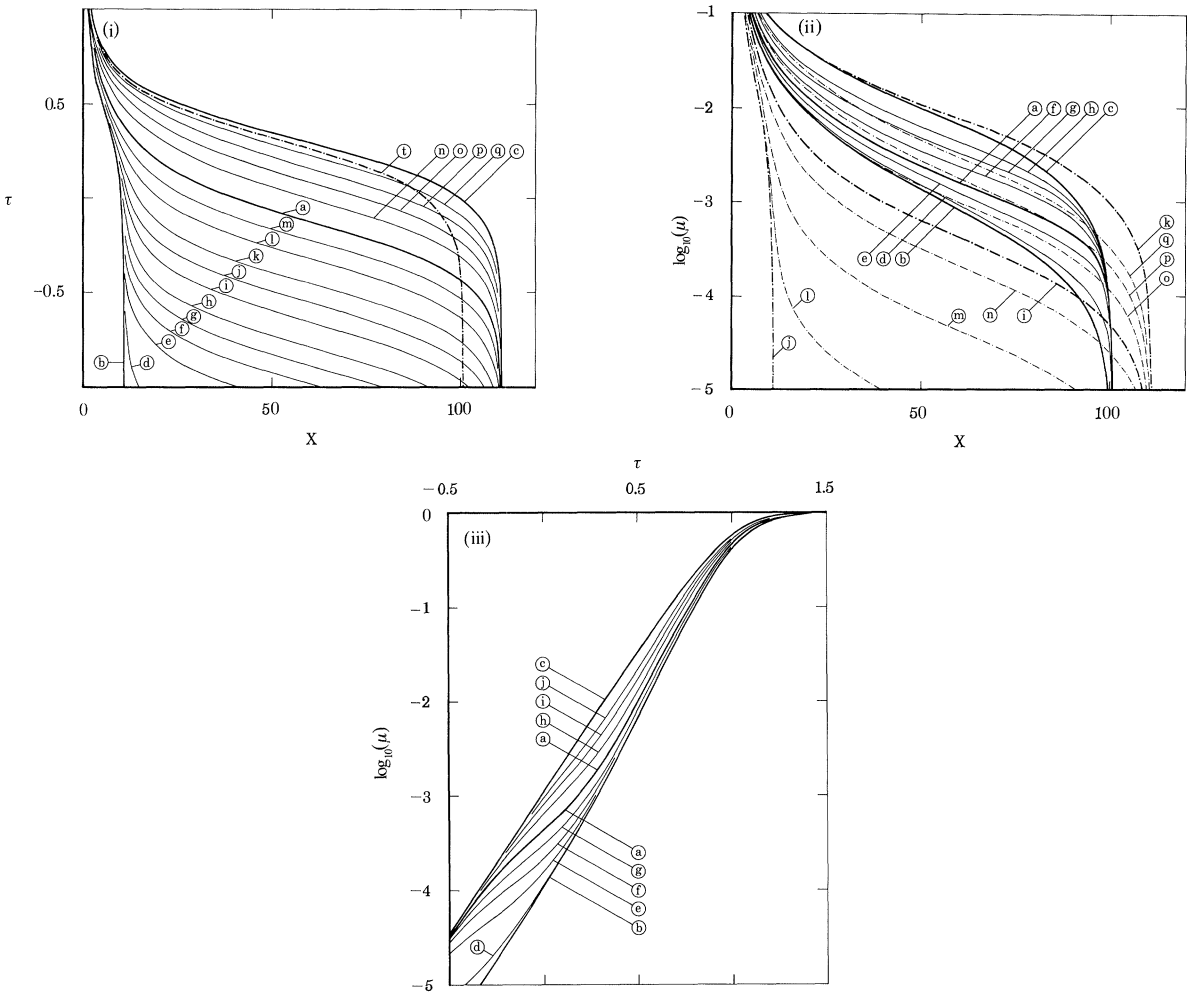

Figure 8. The location of the plastic and self-thinning lines for different values of the plant slenderness ratio λ_∞ for plants in hexagonal packing. All other parameters have the same values as those of figure 7.

(i) The τ–X plane. Plastic lines for values of λ_∞ as follows: (a) 1, (b) 10^{-6}, (c) 10^{6}, (d) 10^{-4}, (e) 10^{-3}, (f) 2.5×10^{-3}, (g) 5×10^{-3}, (h) 10^{-2}, (i) 2.5×10^{-2}, (j) 5×10^{-2}, (k) 10^{-1}, (l) 2.5×10^{-1}, (m) 5×10^{-1}, (n) 2.5, (o) 5, (p) 10, (q) 25. (t) The self-thinning line for all values of λ_∞.

(ii) The log (μ)–X plane. The broken lines represent plastic lines and the solid ones are self-thinning lines. Values of λ_∞ are as follows: (a, i) 1, (b, j) 10^{-6}, (c, k) 10^{6}, (d, m) 10^{-1}, (e, n) 5×10^{-1}, (f, o) 2.5, (g, p) 5, (h, q) 10, (l, plastic line only) 10^{-2}.

(iii) The log (μ)–τ plane. For clarity, only the self-thinning lines are shown (the plastic line is as for figure 7 (iv) and lies slightly below and to the right of line (c) of the present figure). Values of λ_∞ are as follows: (a) 1, (b) 10^{-6}, (c) 10^{6}, (d) 10^{-2}, (e) 10^{-1}, (f) 2.5×10^{-1}, (g) 5×10^{-1}, (h) 2.5, (i) 5, (j) 10.

λ_∞. Both the plastic and thinning lines change position with λ_∞ on the log (μ) $\sim X$ plane, but again, only that of the plastic line becomes altered on the log (μ) $\sim \tau$ plane. In both of these figures there are regions where the mass corresponding to Phase III growth exceeds that for normal natural growth for a given number X of plants.

DIFFUSION OF IDENTITY PROPERTIES ACROSS GROWTH-PHASE BOUNDARIES

In real spacetime the growth-phase boundaries will not be sharply defined. In Phase I, τ and X are virtually independent. In Phase II each plant is unaware of the existence of others because there is no direct physical contact of plant cylinders even when the inevitable variations about the mean dimensions of these cylinders ensures the actual presence of considerable amounts of overlap and overtopping as Phase III is approached. Each plant is only aware of the reduced level of radiation and nutrients available to sustain growth. Both Phases I and II are distinguished by their dependence on the relative availability of radiation and nutrients so that, in theory, each could be induced artificially from the other by suitably augmenting, or diminishing, these quantities. For Phase III the thinning line represents the conditions associated with what amounts to a physical barrier to further unrestricted radial growth. These conditions must therefore always influence growth to a greater or lesser extent, even though this may be an extremely weak influence in some cases, such as for small τ and a sparse population (small X).

When account is taken of the uncertainties in specifying population mean planting density and plant dimensions on the basis of finite samples, by describing

Downloaded from rstb.royalsocietypublishing.org

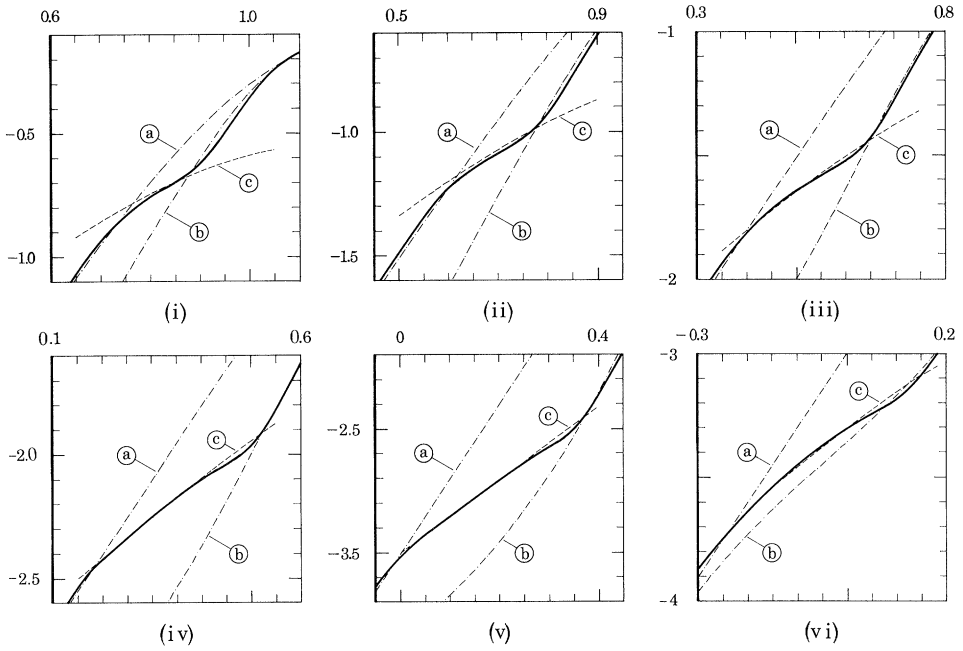

Figure 9. Modification of the growth surface due to the diffusion of identity properties across the growth-phase boundaries. The diagrams (i)–(iv) are enlargements of the corresponding curves shown in figure 7 (iv). The growth life-lines corresponding to these are shown in figure 7 (i) and (ii). Values of parameters are as for figure 7, together with $\sigma_1 = 0.05 = \sigma_2$, $\sigma_3 = 0.1\sqrt{X_0}$, $\sigma_4 = -0.1$, $\Delta\tau = 0.025$. For all cases shown, (a) is the plastic line and (b) is the self-thinning line. (c) Life-lines on the growth surface without diffusion of identity properties; for clarity, these lines are shown extended to regions beyond the plastic and self-thinning lines. The unbroken lines are life-lines with diffusion for initial planting density $X = X_0$ as follows: (i) 3, (ii) 5, (iii) 10, (iv) 20, (v) 40, (vi) 80.

these quantities in terms of a distribution with expectation and variance, the cumulative diffusive effect on the life-line is to round off the approaches to the otherwise sharply defined plastic and self-thinning lines on the growth surface. This rounding is additional to the curvature of these phase boundary lines due to their dependence on time τ and planting density X, and which alone can be quite marked in some cases, as is apparent for small τ and large X in figures 6–8. The diffusion effect is dependent on sample size and will be most pronounced for small samples and least for large ones in accord with their respective variances. In evaluating it, it is necessary to distinguish between the growth non-uniformities evident in log-normal distributions of plant mass, and related quantities, as may exist within a given even-aged stand (Koyama & Kira 1956), and the conditions of strict stand growth uniformity of means specified for the present analysis. Non-uniform stand growth will also lead to rounding of the life-lines near the phase boundaries, but these cases require separate, special treatment, and are not discussed here.

The values of mass $M(t)$ and planting density $X(t)$ used here are overall population characteristics and, as such, represent the expectations of the means of all possible samples of a given size from the totality of similar stands at the same growth state. By the central limit theorem (Papoulis 1984; Hugill 1985), the distribution of such means is asymptotically normal, irrespective of the distributions within the individual stands, and they have accordingly been represented in this way with monovariate and bivariate Gaussian probability density functions. Details of the particular calculation methods used are given in Appendix 3 and some results for one arbitrarily selected set of values for the required statistical parameters are shown in figures 7 and 9. In addition to the rounding, the overshooting of the undiffused life-lines by the diffused ones evident in these figures is also a consequence of the statistical uncertainty of the growth state and planting density, at a given instant, on the actual mass calculated for the solar cylinder. It means that growth life-lines are, in this sense, unique as well as for the reasons mentioned earlier, even though, as loci, they may share a common growth surface with other life-lines having widely different origins.

GROWTH AND THINNING MECHANISMS IN STANDS

There is clearly a need for an examination of the dynamic stability of growth in stands to determine the possible effects on the growth processes and the circumstances in which they arise. Before this is done in detail it is pertinent, and may even be sufficient, to consider some global observations, made on the basis of a quasi-static analysis, of the effects and variation with time of non-uniformities in the masses of plants in stands in the three growth phases. This shows, *inter alia*, some of the consequences of one-sided competition arising from destabilized growth.

There is basically nothing special about Phase I, because there is sufficient space, radiation energy and nutrients for plants to grow naturally in what amounts to isolation. Variations in the sizes of otherwise similar individuals, as measured by the means of samples from the entire population, will occur independently in an asymptotically normal distribution in accord with the

Downloaded from rstb.royalsocietypublishing.org

central limit theorem mentioned earlier. In such conditions of unrestricted growth each plant can increase its biomass by normal root, stem, shoot and foliage growth so that the canopy and root envelopes should have their usual mean shapes. In equation (6) only one of λ_r or λ_h exists independently for a given mass, which means that the proportions of a plant are regulated directly by the energy-conversion process. If the process is destabilized by a reduction $\delta\lambda_r$ in λ_r, compensation is by an increase $\delta\lambda_h$ in the height λ_h given by

$$\delta\lambda_h = -2(\lambda_h/\lambda_r)\,\delta\lambda_r, \tag{41}$$

to first order, and this is marked when $\lambda_h \gg \lambda_r$. A relatively small change in radial dimensions may thus lead, in some cases, to the formation of a spindly plant (see, for example, Weiner *et al.* 1990) with no theoretical restriction on height, save that of its structure becoming too slender to be self-supporting (Givinish, 1986).

In Phase II there are constraints to growth in that the total biomass produced is that of the solar cylinder. This is the supremum of the sum of the masses of the individual plants for each of which growth is no longer independent because of the lack of sufficient usable radiant energy to sustain it. In Phase III there are obvious direct physical constraints to growth, owing to the packing at self-thinning. Phase II growth is therefore the one of immediate interest. In it a redistribution of mass between the members of a stand, after a perturbation from autocatalytic growth equilibrium, may engender a one-sided competition process leading to varying degrees of hierarchical dominance and premature self-thinning, as is shown in the following quasi-static analysis of binary equilibrium mass states. An extension to tertiary and higher-order systems is a trivial matter and not therefore discussed.

For n plants, each of mean mass μ_m, but of different sizes and individual masses μ_j in Phase II growth, the total biomass $\mu_s = n\mu_m$ produced in the stand containing solar cylinders of mean height H is

$$\sum_{j=1}^{n} \mu_j = \mu_s = n\mu_m, \tag{42}$$

where, for autocatalytic growth at time τ, the individual amounts of biomass are

$$\mu_j = 1/\{1+\alpha_j \exp(-\beta_j \tau)\}. \tag{43}$$

As shown earlier, autocatalytic normal growth is unstable to first order for $\tau < 1$, $\mu_j < \frac{1}{2}$, and subsequently stable beyond these limits. In a stand of n plants there are up to $(n-1)$ degrees of freedom for possible non-uniformities of growth, so that if a number k of these n plants is supposed as having uniformly augmented growth, each with biomass μ_a, and that the remaining energy available for conversion in the solar cylinders is shared equally among the others, each with necessarily diminished biomass μ_d, in a hierarchy of exploitation not unlike that referred to by Harper (1967), then

$$\sum_{j=1}^{k} \mu_{a_j} + \sum_{k+1}^{n} \mu_{d_j} = \mu_s, \quad k \leqslant n-1. \tag{44}$$

If these distinct groups each contain members of different equal sizes, μ_a and μ_d, then

$$k\mu_a + (n-k)\,\mu_d = \mu_s, \tag{45}$$

and the diminished biomass μ_d is therefore

$$\mu_d = \mu_s(1-k\mu_a/\mu_s)/(n-k), \tag{46}$$

with

$$\mu_a = 1/\{1+\alpha_a \exp(-\beta_a \tau)\},$$
$$\mu_s = n/\{1+\alpha_m \exp(-\beta_m \tau)\}, \tag{47}$$

where α_m and β_m are as in (23). The initial and intermediate conditions used in evaluating the first of these expressions were

$$\tau = 0, \quad \mu_a = \mu_{a0} + \delta\mu_0; \quad \tau = 1, \quad \mu_a = \mu_{a1}, \tag{48}$$

giving

$$\alpha_a = 1/\mu_{a0} - 1, \quad \beta_a = \ln\{\mu_{a1}\alpha_a/(1-\mu_{a1})\}, \tag{49}$$

where $\delta\mu_0$ and μ_{a1}, are chosen as required.

For the continued existence in Phase II of the $(n-k)$ plants of diminished biomass μ_d it is clear from (46) that $k\mu_a/\mu_s$ must be less than 1, and there is therefore a theoretical boundary separating positive and negative growth rates, defined by $\mu_d'(\tau) = 0$, where the prime denotes differentiation, for which

$$(\beta_m/\beta_a)\,(\mu_s/\mu_a)\,(1-\mu_m)/(1-\mu_a) = k. \tag{50}$$

Negative growth rates can only occur if some part of the growth process as a whole is physically reversible, and strong, healthy plants can actually succeed in causing the biomass of less robust neighbours to become reduced. If this is not so, and the onset of a negative growth rate implies mortality (Aikman & Watkinson 1980; Mahmoud & Grime 1974), then the value of $k = k_{crit}$, which separates the cases that can recover from those that cannot, is given by the lower integer bound $[k_{crit}]$ for k_{crit} on the diminished mass curve with an inflected stationary point defined by $\mu_d'(\tau) = 0 = \mu_d''(\tau)$ and satisfying

$$\mu_s''(\tau) = k\mu_a''(\tau). \tag{51}$$

The value of τ at which this occurs is therefore given by

$$\beta_m(1-2\mu_m) = \beta_a(1-2\mu_a). \tag{52}$$

No plant in already diminished growth can exist beyond the absolute limits $\tau = \tau_{mort}$, obtained as solutions of

$$k\mu_a = \mu_s, \tag{53}$$

because all of the available resources are then accounted for by the plants in augmented growth, in accord with the observations of Firbank & Watkinson (1985). The upper limit for τ_{mort} is fixed by the definitive growth-limit boundary which separates all cases for which recovery is a theoretical possibility, from those for which it is not, and which is defined by evaluating $\tau = \tau^*$ such that the conditions (53) and $\mu_d'(\tau) = 0$ are satisfied. This occurs when

$$\exp\{(\beta_a-\beta_m)\tau^*\} = n\alpha_a\beta_a\mu_a/(\alpha_m\beta_m\mu_s). \tag{54}$$

For this value of $\tau = \tau^*$ the corresponding masses are

Downloaded from rstb.royalsocietypublishing.org

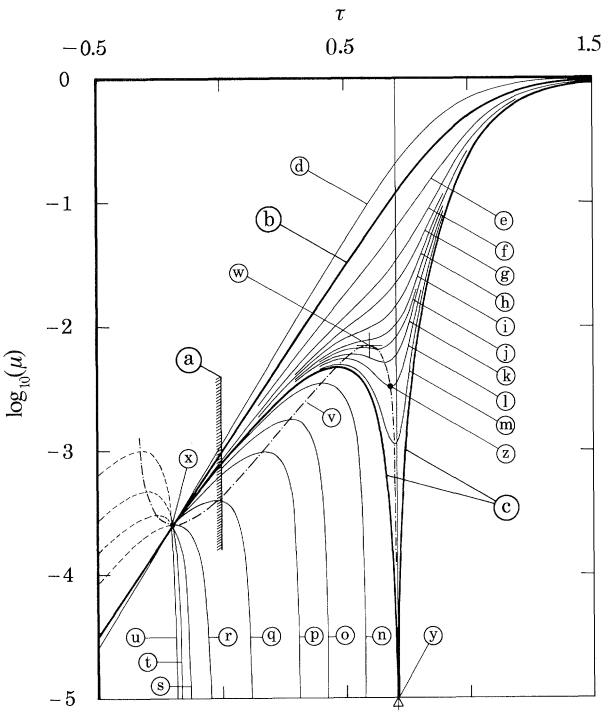

Figure 10. Phase II autocatalytic growth curves for $n = 100$ plants of which k are in uniformly augmented growth and the remainder (n–k) are in uniformly diminished growth at $\tau = 0$. The curves are shown extended to earlier times ($\tau = -0.5$) to indicate the mathematical implications of the assumptions for the augmented and diminished biomass at $\tau = 0$. Parameter values: $\mu_0 = 0.001$, $\delta\mu_0 = 0.15\mu_0$, $\mu_{a1} = 0.7$, $\alpha_m = 999$. (a) Boundary on which initial conditions are specified. (b) Normal Phase II growth curve. (c) Definitive growth limit boundary for which $k = k^* = 58.24499$. Curves below this boundary are for growth terminating at $\tau = \tau_{mort}$. (d) Augmented growth curve for k plants. (e–u) Diminished growth curves for $(100-k)$ plants with k, and τ_{mort} in parentheses, taking the following values: (e) 40, (f) 50, (g) 52, (h) 55, (i) 56, (j) 56.5, (k) 57, (l) 57.5, (m) 58, (n) 60 (0.5754763), (o) 65 (0.4256793), (p) 70 (0.3116574), (r) 90 (−0.0483178), (s) 95 (−0.1252451), (t) 97.5 (−0.1619852), (u) 99 (−0.1835758). (v) Boundary separating positive and negative growth rates. (w) Local maximum on the boundary (v) and consistent with the diminished mass curve satisfying $\mu_d'(\tau) = 0 = \mu_d''(\tau)$ and for which $k_{crit} = 56.33892$, $[k_{crit}] = 56$, $\tau = 0.6012254$, $\log(\mu) = -2.149923$. (x) Point of intersection at $\tau = -0.1977875$ satisfying $\mu_a = \mu_d$. This point is independent of both n and k. (y) The definitive growth limit line $\tau - \tau^* = 0.7041525$. (z) Local minimum representing the current mass of a nearly dead tree and with its subsequent recovery to normality occurring with increase in τ.

μ_{a1} and μ_{s1} and this, in turn, means that, for a given n, the number $k = k^*$ of plants in uniformly augmented growth on this boundary is given by

$$k^* = \mu_{s1}/\mu_{a1}. \qquad (55)$$

Simple iteration was used for dealing with the implicit forms of the preceding equations in obtaining the results shown in figure 10, which are for a specified status of growth at time $\tau = 0$. The figure also shows what would have been the case at earlier times for the same growth status at $\tau = 0$, and also what happens in cases like those of the recovery to normal, or near-normal, stature for trees for which the amount of living tissue has become reduced by circumstances to a smaller-than-usual amount. Cases involving greater degrees of non-uniformity in biomass may be dealt with in much the same way and will lead to similar conclusions for continued existence and for theoretically negative growth rates (J. L. Harper, personal communication, 21 June 1989).

Phase II growth is thus either reduced normal and stable, with life-lines on the growth surface of the kind shown in figure 6, or it is non-uniform and unstable to a degree, and with life-lines modified accordingly. Reduced normal growth may involve variations in height, radius and limb sizes, either separately, or in combination, to account for the alteration in biomass (Weiner *et al.* 1990). When there is unstable growth such deformative processes may well be wholly or partly resisted by strong, healthy plants; in these circumstances, premature death of the weaker ones must be regarded as a normal consequence of maintaining an energy–biomass production equilibrium. Such an instability mechanism, with or without mortality, is a suitable one for the establishment of clumps.

Phase III growth is an altogether different matter because the occurrence of physical contact between adjacent plant cylinders means that the instantaneous limit for radial growth has been reached. Further radial growth is possible only if space becomes available for it by the removal of neighbouring cylinders. When this is achieved by self-thinning the question of immediate interest is whether or not such a process is an entirely haphazard one, one of progressive rearrangement from an initial pattern of inferior packing efficiency to an improved one, one of preserving an already optimum arrangement, or any combination of these (Greig-Smith 1964). Figure 11 shows idealized sequences in possible thinning processes in which live plants are always surrounded by dead ones at any stage, which is consistent with observations made by Cannell *et al.* (1984). These discrete sequences correspond to the progressive doubling in size of plant cylinder radii for each of three packing arrangements. For the close-packed hexagonal pattern, symmetry is shown as being preserved during progressive growth stages by removal of families of plants disposed on concentric annular rings. For the square-packed arrangement the thinning is according to the alternating pattern of positions on concentric annular rings as indicated in the figure, whereas the haphazard pattern is shown progressing towards the optimum close-packed hexagon. At any intermediate time, such as during the initially over-thinned final stage when only one plant occupies the solar cylinder, there may be a temporary reversion to Phase II, or even to Phase I, growth if the available resources are adequate. In each case the central plant is the only one ultimately to remain in the solar cylinder, but this is unimportant for large stands because the choice of any one ultimate survivor as origin well away from the stand boundaries is legitimate. For stands involving smaller numbers of plants on an otherwise open plane the non-uniform competition for the available resources on the inside

PHILOSOPHICAL TRANSACTIONS OF THE ROYAL SOCIETY B BIOLOGICAL SCIENCES
PHILOSOPHICAL TRANSACTIONS OF THE ROYAL SOCIETY B BIOLOGICAL SCIENCES

Downloaded from rstb.royalsocietypublishing.org

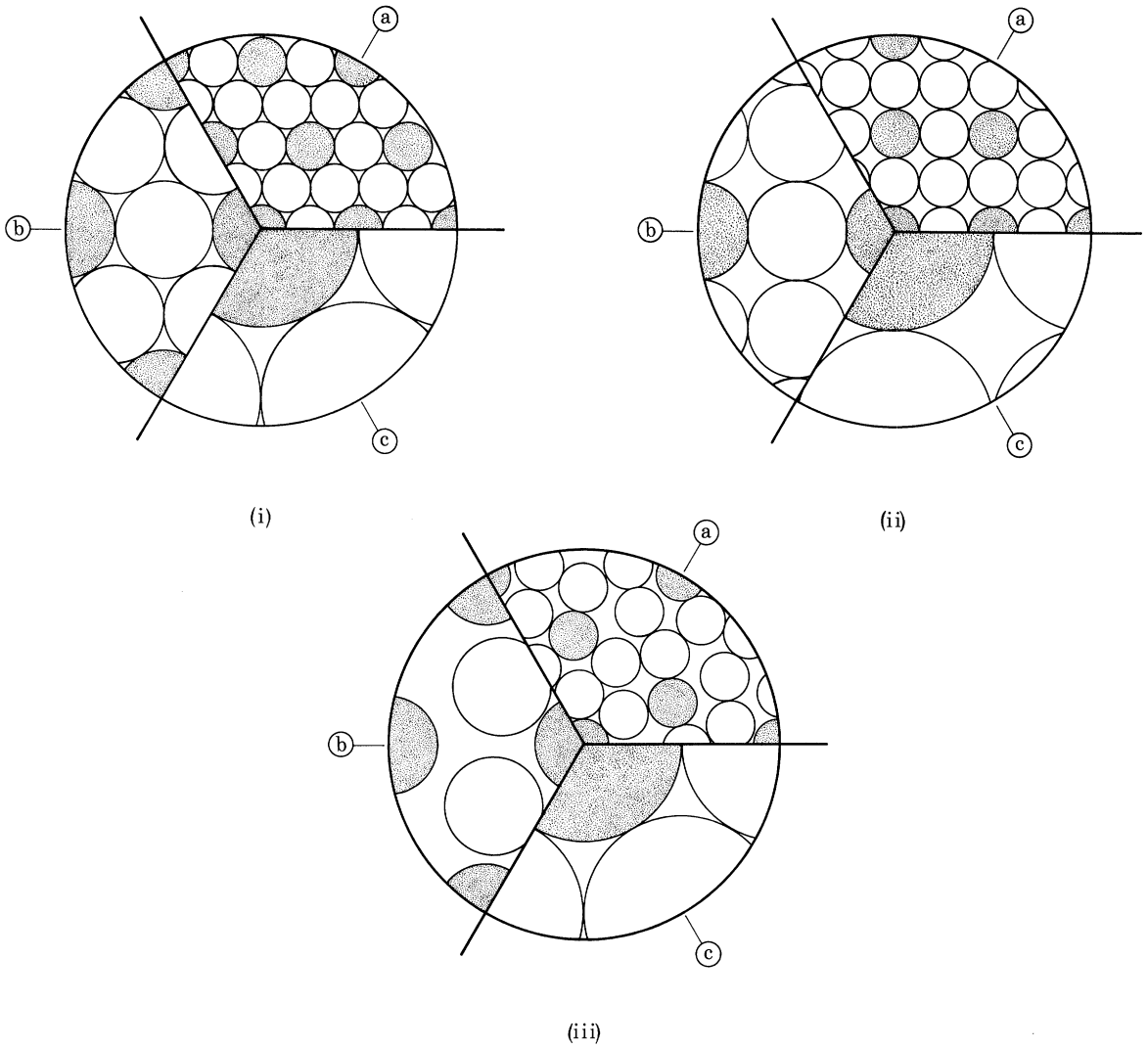

Figure 11. Possible stages in the relative locations of plants during self-thinning. In each of the diagrams (i)–(iii) the outer circle represents the periphery of the solar cylinder and the smaller circles those of the plant cylinders. Each diagram shows three stages in the process from an initial arrangement in the sectors labelled (a) and progressing by the sequential doubling of plant cylinder diameters to new arrangements at (b) and (c). Ultimately, only the plant initially at the centre of each arrangement exists to fill completely the solar cylinder. The plants whose existence at any one stage continues to at least one stage further are represented by the shaded circles and the currently doomed plants by the unshaded ones.

(i) Close-packed hexagon pattern preserved at all stages. This symmetry is preserved by the demise of families of plants on concentric annular rings. (a) Initial stage. (b) First intermediate stage. (c) Second intermediate stage, which is one stage removed from the complete filling of the solar cylinder.

(ii) Close-packed square pattern preserved at all stages. Thinning proceeds in this case by the demise of an alternating pattern of plants on concentric annular rings. (a–c) stages as for (i).

(iii) Arbitrary initial pattern. The three stages shown indicate progress during self-thinning towards the uniform close-packed hexagonal arrangement, which provides the optimum density on the plane of cultivation.

and outside of the stand perimeter must be taken into account.

DISCUSSION

There is apparently no immediate supply of experimental data in the form required for comparison with the foregoing analytical work in all of its detail. For Phases I and II this is relatively unimportant because little more need be said of autocatalytic growth in these two phases other than noting that instabilities leading to non-uniformities and self-thinning at later times have their origin in Phase II, or perhaps exceptionally in Phase I, when local conditions within an otherwise uniform stand may amount to a pocket of Phase II growth. The significance of such instabilities is that an initial infinitesimal increase, and subsequent augmentation, of the biomass of one or more plants, balanced by compensating reductions elsewhere, leads naturally to the development of one-sided competition. The property may be regarded as one of the more, if not most, important features of stand growth and self-thinning in that some plants may cease to exist before the Phase III boundary is reached. Competition processes of this kind would appear, therefore, to become established before there is physical

PHILOSOPHICAL TRANSACTIONS OF THE ROYAL SOCIETY B BIOLOGICAL SCIENCES
PHILOSOPHICAL TRANSACTIONS OF THE ROYAL SOCIETY B BIOLOGICAL SCIENCES

Downloaded from rstb.royalsocietypublishing.org

contact between the enclosing cylinders of neighbouring plants and hence before there is any overlap of canopy mean radii. Developments subsequent to such overlap (Gates *et al.* 1979), and from overtopping and competition for light (Ford & Diggle 1981), although clearly of significance in Phase III growth, have not been discussed because they are strictly outside the scope of the present work.

For Phase III growth the available field observations have been, on the whole, expressed in terms of either the amount of biomass M produced per plant, or M_g per unit area of ground, and the number of plants X_g situated on this area at stages during the growth process, or the equivalent of these quantities. Attention has been focused on assigning suitable value to the constants a and b in a power law of the form

$$M = aX^b, \tag{56}$$

with some evidence apparently in support of the value $b = -\frac{3}{2}$, as originally proposed for the self-thinning rule (Yoda *et al.* 1963; White & Harper 1970), but there is little agreement as to what value a should take. This is not surprising because (56) is at best able only to offer a partial description of events on the growth surface, and then only in terms of their projection on to the $M \sim X$ plane as has been indicated in figure 6. It is therefore clear that such a law has no place other than perhaps as an approximation of possible utility in some rather restricted circumstances. To show why this is so in detail, and why also considerable variations are to be expected in the values of a and b in (56) when such a law is being used, the dimensional and functional forms of (9) and (10) are now considered.

At any time t in Phase III growth the functional form for the mass M is

$$M = M\{t, X(t)\}, \tag{57}$$

so that the rate of change of biomass with time, $\mathrm{d}M/\mathrm{d}t$, is

$$\mathrm{d}M/\mathrm{d}t = \partial M/\partial t + (\partial M/\partial X)\,(\partial X/\partial t). \tag{58}$$

It is immediately clear from (58), and also from figure 6, that the quantity $\partial M/\partial X$ cannot be taken in isolation in the form bM/X derived from (56) unless the restrictions implied by doing this are acceptable, and in most cases of interest they are not. This rules out the possible existence of a unique value $b = -\frac{3}{2}$ (Ford 1975; Lonsdale 1990), and also of a, for reasons which become clear when the dimensional form of the Phase III mass equation is considered.

When the mean biomass per plant M, and the number of plants X, in the solar cylinder are expressed as fractions M_g and X_g respectively of an arbitrarily selected ground reference area S_g, sufficient to accommodate N_g solar cylinders, the relations between these quantities are

$$M_g = MN_g X/S_g \tag{59}$$

and

$$X_g = N_g X/S_g. \tag{60}$$

These define the biomass and number of plants per unit area of ground respectively. Three combinations, $M \sim X$, $M \sim X_g$, and $M_g \sim X_g$, of these quantities are of interest and are now considered in that order.

Case 1. $M \sim X$

From (10), with $M_3 = M$ and $X_t = X$,

$$M = (M_\infty \sigma \Lambda)\,(\lambda_h/X)\,(\lambda_\infty + 2\lambda_h)/ \{\lambda_\infty + 2\lambda_h (X/C_p)^{\frac{1}{2}}\}, \tag{61}$$

and, on the self-thinning line, $X = C_p/\lambda_r^2$. Taking logarithms (as was done for similar reasons by Perry 1984) this equation becomes

$$Z_1 = A + B(t) - Y_1 - \ln\{\lambda_\infty + C(t)\exp(Y_1/2)\}, \tag{62}$$

where

$$Z_1 = \ln(M), \quad Y_1 = \ln(X), \quad A = \ln(M_\infty \sigma),$$
$$B(t) = \ln\{\Lambda\lambda_h(\lambda_\infty + 2\lambda_h)\}$$

and

$$C(t) = 2\lambda_h/C_p^{\frac{1}{2}}.$$

To interpret (62) in terms of the power law (56) the equivalents of the slope b and intercept a are required. The 'slope' $\partial Z_1/\partial Y_1$ of (62) is

$$\partial Z_1/\partial Y_1 = -(1+\theta), \tag{63}$$

where $\theta = 1/(\theta_1 + 2)$, $\theta_1 = \lambda_\infty \lambda_r/\lambda_h = (\lambda_\infty/\lambda_h)(C_p/X_t)^{\frac{1}{2}}$, and $\lim_{\lambda_\infty \to 0}\theta = \frac{1}{2}$, $\lim_{\lambda_\infty \to \infty}\theta = 0$. The 'slope' thus has a time dependence apparent in the packing coefficient C_p, and also in the quantities λ_r and λ_h, except for the special case of complete geometric similarity during growth and for which the ratio λ_r/λ_h is constant. The 'slope' also depends on the plant slenderness ratio λ_∞, which is a species-class-dependent parameter, defined by canopy-envelope geometry, as distinct from a species-dependent one. The dependence is such that for given values of planting density X and of λ_h and λ_∞, the magnitude of the slope decreases with increase in the packing efficiency defined by C_p, and, for given values of planting density X and of C_p and λ_∞, it increases with increase in relative height λ_h.

The equivalent of the 'intercept' is the value taken by Z_1 when $X = 1$, which is also when λ_r, λ_h and C_p are all unity. This value is

$$Z_1 = \ln(M_\infty \sigma \Lambda) = \ln\{\pi F(t)\rho_\infty R_\infty^2 H_\infty \sigma \Lambda\}, \tag{64}$$

and is clearly not unique because it depends on the fertility function $F(t)$, the biomass density ratio σ which, in turn, depends on the availability of usable radiation, the ultimate value of plant cylinder volume $\pi R_\infty^2 H_\infty$ and the canopy shape parameter Λ, which may have a significant time dependence at some stage of growth.

Case 2. $M \sim X_g$

For this case the mass equations are the same as (61) and (62) but with X replaced by $X = X_g S_g/N_g$. With $Z_2 = \ln(M)$ and $Y_2 = \ln(X_g)$, the 'slope' $\partial Z_2/\partial Y_2$ is the same as $\partial Z_1/\partial Y_1$, but the self-thinning lines contain ordinates $Z_2 = \ln(M_\infty \sigma \Lambda)$, having abscissae $X_g = N_g/S_g$, not $X_g = 1$, but which correspond to $X = 1$. This means that, for a given $(M_\infty \sigma \Lambda)$, extrapolation to $X_g = 1$ defines 'intercept' values which increase with

Downloaded from rstb.royalsocietypublishing.org

the ratio N_g/S_g, as would occur, for example, with either or both a reduction in radial dimensions and/or an increase in the packing coefficient C_p. The amount of this increase is $b \ln (N_g/S_g)$ for a self-thinning line of 'slope' $-b$. This undesirable effect is a direct consequence of the selection of the number of plants X_g per unit area of ground as a unit of measurement without reference to the composition of the whole, or partial, growth components in that area. To make such a selection is to ignore the significance of the very different physical scales involved in the whole range of plant species. As long as the above- and below-ground environments may be regarded as continua then the appropriate physical reference scale for a given plant is a characteristic dimension of that plant, not an arbitrarily selected and unrelated one like S_g.

Case 3. $M_g \sim X_g$

For the third case, (59) and (60) give $M_g = MX_g$, and with $Y_3 = \ln (X_g)$ the 'slope' becomes $\partial Z_3/\partial Y_3 = \partial Z_1/\partial Y_1 + 1$. The corresponding 'intercept' is $Z_3 = \ln (M_\infty \sigma \Lambda)$, as for case 1.

In the substantial literature on, *inter alia*, the possible viability of a power law of the form (56), and the values its 'constants' should take (see, for example, White 1981; Weller 1987; Lonsdale 1990), little attention seems to have been given to the need for grouping the variables required to describe the temporal and spatial sequences of growth events in a suitable non-dimensional form so that the law itself should become, as far as is possible, one of universal application. One such grouping has been dealt with here and the results obtained with it permit a number of observations on several points of interest.

It is clear that a universal power law of the form (56) cannot be defined to describe self-thinning lines, although it may be of some use as an approximation for individual cases, and perhaps more generally for some restricted time intervals and plant class groupings involving similarities of growth, form and environment. The sort of differences to be expected in the slope $\partial Z/\partial Y$ (which is the logarithmic equivalent of $\partial M/\partial X$) of the curve (62) are indicated by the limiting values taken by (63). These are:

(i) $\lim_{\lambda_\infty \to 0} (\partial Z/\partial Y) = -\frac{3}{2}$,

(ii) $\lim_{\lambda_h/\lambda_r \to \infty} (\partial Z/\partial Y) = -\frac{3}{2}$,

(iii) $\lim_{\lambda_\infty \to \infty} (\partial Z/\partial Y) = -1$,

(iv) $\lim_{\lambda_h/\lambda_r \to 0} (\partial Z/\partial Y) = -1$,

(v) $\lim_{\lambda_\infty \lambda_r/\lambda_h = 1} (\partial Z/\partial Y) = -\frac{4}{3}$,

with the addition of $+1$ to all of these quantities for Case 3. When growth proceeds with geometric similarity ($\lambda_r/\lambda_h = 1$) then the upper and lower limit bounds are -1 and $-\frac{3}{2}$ respectively.

Of these limits, $\lambda_\infty \to 0$ corresponds to plants which, at maturity, are extremely tall and very slender;

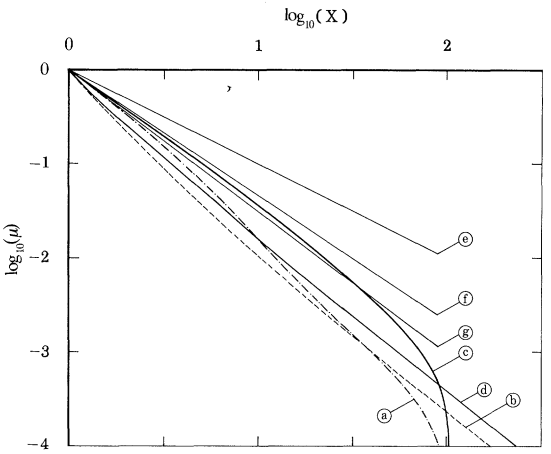

Figure 12. The projection of the plastic and self-thinning lines for autocatalytic growth with hexagonal packing onto the $X \sim \mu$ plane. Parameter values as for figure 7. (a) Plastic line. (b) Plastic line for growth with geometric similarity. (c) Self-thinning line. (d) Self-thinning line for growth with geometric similarity. (e–g); lines of slope -1, $-\frac{4}{3}$, $-\frac{3}{2}$, respectively. All lines pass through (0, 0).

$\lambda_h/\lambda_r \to \infty$ is for a period in the growth time of plants wherein the relative height growth far exceeds the corresponding radial one; $\lambda_\infty \to \infty$ is for plants which at maturity have very large radial dimensions compared with their height; $\lambda_h/\lambda_r \to 0$ is for plants for which the relative radial growth far exceeds that for height during some part of their growth time, and $\lambda_\infty \lambda_r/\lambda_h = R_\infty R/(H_\infty H) = 1$ is for plants of constant and equal radius and height. Together with the case for growth with geometric similarity, these limiting values represent the sort of range to be expected in the 'slope' of the self-thinning line when it is evaluated in this way.

Figure 12 shows the plastic and self-thinning lines of figure 7 (iii) to logarithmic scales, together with lines of slopes -1, $-\frac{4}{3}$, and $-\frac{3}{2}$. Because all the lines in this figure are projections from the growth surface on to the $\mu \sim X$ plane (plane (*c*) of figure 6), due regard should be given to the implicit dependence on time, for this alone accounts for much of the variation in curve shape for some regions. For example, the self-thinning line for autocatalytic growth is seen to follow the line of slope $-\frac{3}{2}$ for much of its length but has markedly increased slope at the larger values of X. This is because of the constraints imposed by the packing and the increasing dependence of biomass on the non-dimensional time τ as the planting density X approaches the maximum possible for the particular parameter values selected for this curve. The source of this varying functional dependence is evident in (58) and can be seen in figure 6. It is the sort of variation in 'slope' to be expected and, as such, does much to explain the corresponding observed variations reported in the literature (see, for example, Weller 1987; Lonsdale 1990). Although such an increase is absent from the curve shown for growth with geometric similarity, it is extremely unlikely that this particular description of growth form can exist in other than special circumstances and at restricted values of planting density X. At large values of X alterations of slope are, more or less, bound to occur in any case. The intercepts ($t \to \infty$) of all curves on figure

PHILOSOPHICAL TRANSACTIONS OF THE ROYAL SOCIETY B BIOLOGICAL SCIENCES
PHILOSOPHICAL TRANSACTIONS OF THE ROYAL SOCIETY B BIOLOGICAL SCIENCES

Downloaded from rstb.royalsocietypublishing.org

12 are zero because of the removal of the species-dependent parameters M_∞, σ and Λ in forming the non-dimensional mass ratio μ.

In general terms, the dependence of the power law 'intercept' on radiation, size and canopy shape, severally and jointly, has also been reported and discussed elsewhere (see, for example, Ford 1975; Harper 1977; White 1981; Westoby & Howell 1986; Lonsdale & Watkinson 1982, 1983; Perry 1984; Lonsdale 1990). The present analysis shows the origin of this dependence for, with the 'intercept' defined by $Z = \ln(M_\infty \sigma \Lambda)$, which is augmented by the quantity $b \ln(N_g/S_g)$ for a self-thinning line of 'slope' $-b$ in the coordinate system $M \sim X_g$, the physical features affecting the values it takes are immediately obvious. The magnitude of the 'intercept' increases with increase in the biomass density ratio σ for a given value of $M_\infty \Lambda$, owing to an increase in the availability of usable radiation energy. This is consistent with reported observations on the effects of varied light intensities (White & Harper 1970; Westoby & Howell 1986). If such a variation occurs with time it may result in a marked increase in the rate at which self-thinning occurs (Clark 1990), because an increase in μ at a given time τ means an increase in λ_h and λ_r. The constraint (9) imposed by the self-thinning conditions thus requires a corresponding reduction in X for this value of τ. The magnitude of the 'intercept' also increases with increase in Λ for a given $M_\infty \sigma$, which occurs with changes in canopy geometry to a form which fills more completely the plant cylinder, and it also increases with increase in the ultimate mass M_∞ for a given $\sigma\Lambda$.

When the composition of the mass term M_∞ is considered, the effects of differing canopy geometries becomes clear. For two different monocultures, each having the same ground reference area S_g, and each containing the same number N_g of plant cylinders, all of which are in contact and subject to self-thinning along a line of 'slope' $-b$, the 'intercept' term for both has the form

$$Z = \ln\{M_\infty \sigma \Lambda (N_g/S_g)^{\frac{3}{2}}\}. \quad (65)$$

If the packing densities, N_g/S_g, and arrangements are also the same for both, so that the radii R and packing coefficients C_p are separately equal, the difference between their 'intercepts' Z, for equal fertility $F(t)$ and biomass density ratio σ, is, with the cases distinguished by the suffices 1 and 2,

$$Z_1 - Z_2 = \ln\{H_{\infty 1} \Lambda_1 / H_{\infty 2} \Lambda_2)\} = \ln\{\lambda_{\infty 2} \Lambda_1 / (\lambda_{\infty 1} \Lambda_2)\}. \quad (66)$$

This result shows that the product of height and shape parameter defines the relative placing of the thinning line in power-law interpretations in that, relative to a comparative datum canopy $(H_{\infty 2} \Lambda_2)$, the intercept becomes increased or decreased according as the ratio $(H_\infty \Lambda_1)/(H_{\infty 2} \Lambda_2)$ is greater or less than unity. It also shows that, for canopies having the same shape parameter, such an increase or decrease will be in accord with the height ratio $H_{\infty 1}/H_{\infty 2}$, which is the same as the ratio $\lambda_{\infty 2}/\lambda_{\infty 1}$ for plants of equal mean radius R_∞. For canopies of the same mean height and common radii the greatest possible increase is defined when the shape parameter Λ_1 takes its maximum value of unity.

In principle, these observations are in accord with the existence of a topological series as proposed by Harper (1977, p. 187), but not entirely so in matters of detail and inferred sequential order. This is because the ordering mentioned by Harper (1977) was based on the relative placing of 'intercepts' defined in terms of useful timber volumes obtained from a given number of trees per acre, rather than for biomass in the sense used here. The canopy geometries considered varied between the 'strikingly pyramidal' one of *Abies nobilis*, and the 'round-crowned' ones of sycamore, ash and birch, as extremes. The actual differences between the 'intercepts' for these cases cannot be evaluated because the required parameters, λ_∞ and Λ, are not known, but it is possible to make estimates, by using (66), which show the trends involved. Suitable simple cases for this purpose are those of a hemispherical crown as datum and, for comparison, a parabolic one of varied height and hence varied $\lambda_{\infty 1}$, both with flat bases of the same diameter at ground level. For the hemispherical crown $\lambda_{\infty 2} = 1$ and $\Lambda_2 = \frac{4}{9}$, and for a parabolic canopy (like that of *Abies nobilis*, for which $\lambda_\infty \approx 0.2$), $\Lambda_1 = 0.28$. In these circumstances (66) becomes $Z_1 - Z_2 = \ln(0.63/\lambda_{\infty 1})$, so that the demarcation between positive and negative differences occurs at $\lambda_{\infty 1} = 0.63$. Values of $0.63/\lambda_{\infty 1}$, which define one intercept as a multiple of the other, are as follows.

$\lambda_{\infty 1} = \frac{R_{\infty 1}}{H_{\infty 1}}$	0.050	0.100	0.200	0.400
$\frac{0.63}{\lambda_{\infty 1}}$	12.60	6.300	3.150	1.575
$\lambda_{\infty 1} = \frac{R_{\infty 1}}{H_{\infty 1}}$	0.600	0.800	1.000	
$\frac{0.63}{\lambda_{\infty 1}}$	1.050	0.788	0.630	

The variations in 'intercepts' evident in this table confirm Harper's proposition. They are also comparable with those of the wide range referred to by White (1981), but even greater variations would emerge as a result of increasing the ratio Λ_1/Λ_2, and also of including the canopy base height H_0. Variations of this kind are consequences of the retention of dimensional forms for the presentation and analysis of field observations. They do not represent fundamental differences in growth processes and they vanish when suitable non-dimensional groupings of quantities are made. Such groupings provide a means of identifying the parameters of significance and the true dependence and interrelation between them. When this has been achieved the establishment of such universal laws as may exist then becomes a viable proposition.

CONCLUDING REMARKS

The unified non-dimensional results that have been established describe primary features of three of the

PHILOSOPHICAL TRANSACTIONS OF THE ROYAL SOCIETY B BIOLOGICAL SCIENCES
PHILOSOPHICAL TRANSACTIONS OF THE ROYAL SOCIETY B BIOLOGICAL SCIENCES

Downloaded from rstb.royalsocietypublishing.org

known growth phases without obscuring these in any way with matters of secondary, but otherwise important, detail. As such they provide a fundamental basis for the development of theoretical work, which takes account of within-canopy detail and root growth, and they also show how the various descriptive dimensions can be combined for the reduction of experimental observations to meaningful non-dimensional forms. For these the biomass $M(t)$, together with plant cylinder height H and radius R, must be expressed in terms of their statistical mean values at time t in conditions of adequate nutrition and radiation for normal healthy growth to an ultimate mean mass M_∞, and height H_∞, on a ground reference area πR_∞^2. In the non-dimensional grouping, the biomass density ratio $\sigma = \rho_s/\rho_\infty$, which accounts for differing levels of radiation, and the canopy shape parameter Λ, are combined with the mass M_∞, thereby reducing the number of variables defining the growth surface. As the canopy shape parameter depends on plant geometry rather than species, there is a need to establish a suitable classification of plants into groups for which it takes similar values. The shape parameter is not a difficult one to evaluate for relatively well-defined canopy geometry, as is the case for many trees and shrubs, particularly when the volume enclosed by the canopy is well packed with branches and shoots, but for more open arrangements of limbs, and especially for soft and flexible ones, the actual geometry to be taken in defining it is less easy to determine. For these cases a combination of the angles between main stem axes and the lengths of limbs, assumed to be straight, emanating from them permits a definition of canopy envelope geometry which may be acceptable, at least in the first instance. In completing the required non-dimensional grouping with the specification of the biomass density ratio σ, there may be a case for evaluating the combination $(\sigma\Lambda)$, rather than either one of the two components in isolation, because this quantifies the end-result of the energy–biomass conversion process in the sense in which it has been used here.

There is also a need to establish suitable values for the statistical parameters defining diffusion at the growth-phase boundaries so that reliable estimates can be made of the amount of rounding of the life-lines to be expected at these boundaries in given cases. As a matter of fine detail, these parameters are also required for estimating the supremum for normal natural growth which, in the analytical sense, determines the optimum spacings for plantings requiring completely normal growth at all future times. For the different from normal growth conditions of Phases II and III the associated alterations to plant architecture, and the manner in which these take place, need to be evaluated systematically for different species, planting arrangements, and environments.

Although the growth behaviour and dynamic response of multicultures to local variations in biomass have not been discussed, there are at least two advantages, in addition to the obvious ones, to be derived from mixed plantings of species with significantly different half-life times $t_{\frac{1}{2}}$. First, for plants of nominally equal heights $H(t)$, the amount of biomass produced can be augmented by filling up the otherwise empty spaces in the packing distribution at self-thinning. Secondly, for plants in normal growth, with canopies having a well-defined base line sufficiently far above ground level, there is likely to be an excess of radiant energy available for alternate use and the total volume in the plant cylinder need no longer be regarded as inviolable. In these circumstances a second undepleted culture may coexist with the primary occupant of the cylinder, with perhaps further repetition of this kind of arrangement to lower size orders and increasing amounts of shade.

This work arose from discussions and correspondence with Professor J. L. Harper, whose help and guidance are gratefully acknowledged. Gratitude is also expressed to referees for their most helpful comments.

REFERENCES

Aikman, D. P. & Watkinson, A. R. 1980 A model for growth and self-thinning in even-aged monocultures of plants. *Annls Bot.* **45**, 419–427.

Assmann, E. 1970 *The principles of forest yield study*. Oxford: Clarendon Press.

Barreto, L. S. 1990 *SPESS; a simulator for pure even-aged stands*. Universidade Tecnica de Lisboa, Instituto Superior de Agronomia, Departamento De engenharia Florestal.

Bazzaz, F. A. & Harper, J. L. 1976 Relationship between plant weight and numbers in mixed populations of *Sinapsis alba* (L.) and *Lepidium sativum* (L.). *J. appl. Ecol.* **13**, 211–216.

Bertanlanffy, L. von 1941 Stoffwechseltypen und Wachstumstypen. *Biol. Zbl.* **61**, 510–532.

Bertalanffy, L. von 1957 Quantitative laws in metabolism and growth. *Q. Rev. Biol.* **32**, 217–231.

Cannell, M. G. R., Rothery, P. & Ford, E. D. 1984 Competition within stands of *Picea sitchensis* and *Pinus contorta*. *Annls Bot.* **53**, 349–362.

Charles-Edwards, D. A. 1984*a* On the ordered development of plants. 1. An hypothesis. *Annls Bot.* **53**, 699–707.

Charles-Edwards, D. A. 1984*b* On the ordered development of plants. 2. Self-thinning in plant communities. *Annls Bot.* **53**, 709–714.

Clark, J. S. 1990 Integration of ecological levels: individual plant growth, population mortality and ecosystem processes. *J. Ecol.* **78**, 275–299.

Firbank, L. G. & Watkinson, A. R. 1985 A model of interference within plant monocultures. *J. theor. Biol.* **116**, 291–911.

Ford, E. D. 1975 Competition and stand structure in some even-aged plant monocultures. *J. Ecol.* **63**, 311–333.

Ford, E. D. & Diggle, P. J. 1981 Competition for light in a plant monoculture modelled as a stochastic process. *Annls Bot.* **48**, 481–500.

Gates, D. J., O'Connor, A. J. & Westcott, M. 1979 Partitioning the union of discs in plant competition models. *Proc. R. Soc. Lond.* A **367**, 59–79.

Givinish, T. J. 1986 Biomechanical constraints on self-thinning in plant populations. *J. theor. Biol.* **119**, 139–146.

Gorham, E. 1979 Shoot height, weight and standing crop in relation to density of monospecific plant stands. *Nature, Lond.* **279**, 148–150.

Gompertz, B. 1825 On the nature of the function expressive of the law of human mortality. *Phil. Trans. R. Soc. Lond.* **115**, 513–585.

PHILOSOPHICAL TRANSACTIONS OF THE ROYAL SOCIETY B BIOLOGICAL SCIENCES

PHILOSOPHICAL TRANSACTIONS OF THE ROYAL SOCIETY B BIOLOGICAL SCIENCES

Downloaded from rstb.royalsocietypublishing.org

Greig-Smith, P. 1964 *Quantitative plant ecology* (2nd edn). London: Butterworth.
Harper, J. L. 1967 A Darwinian approach to plant ecology. *J. Ecol.* **55**, 247–70.
Harper, J. L. 1977 *The population biology of plants*. London: Academic Press.
Hozumi, K. 1977 Ecological and mathematical considerations on self-thinning in even-aged pure stands. I. Mean plant-weight-density trajectory during the course of self-thinning. *Bot. Mag., Tokyo* **90**, 165–179.
Hozumi, K. 1980 Ecological and mathematical considerations on self-thinning in even-aged pure stands. II. Growth analysis of self-thinning. *Bot. Mag., Tokyo* **93**, 149–166.
Hugill, M. 1985 *Advanced statistics*. London: Unwin Hyman.
Hunt, R. 1982 *Plant growth curves*. London: Edward Arnold.
Hutchings, M. J. 1983 Ecology's law in search of a theory. *New Scient.* **98**, 765–767.
Hutchings, M. J. & Budd, C. S. 1981 Plant competition and its course through time. *BioScience* **31**, 640–645.
Kays, S. & Harper, J. L. 1974 The regulation of plant and tiller density in a grass sward. *J. Ecol.* **62**, 97–105.
Kira, T., Ogawa, H. & Sakazaki, N. 1953 Intraspecific competition among higher plants. I. Competition-yield-density interrelationship in regularly dispersed populations. *J. Polytechn. Inst., Osaka City Univ.* D **4**, 1–16.
Koyama, H. & Kira, T. 1956 Intraspecific competition among higher plants. VIII. Frequency distribution of individual plant weight as affected by the interaction between plants. *J. Polytechn. Inst., Osaka City Univ.* D **7**, 673–694.
Lonsdale, W. M. 1990 The self-thinning rule: dead or alive? *Ecology* **71** (4), 1373–1388.
Lonsdale, W. M. & Watkinson, A. R. 1982 Light and self-thinning. *New Phytol.* **90**, 431–445.
Lonsdale, W. M. & Watkinson, A. R. 1983 Plant geometry and self-thinning. *J. Ecol.* **71**, 285–297.
Mahmoud, A. & Grime, T. P. 1974 A comparison of negative relative growth rates in shaded seedlings. *New Phytol.* **73**, 1215–1219.
Malmberg, C. & Smith, H. 1982 Relationship between plant weight and density in mixed populations of *Medicago sativa* and *Trifolium* pratense. *Oikos* **38**, 365–368.
Medawar, P. B. 1945 Size, shape and age. In *Essays on growth and form* (ed. W. E. Le Gros Clark & P. B. Medawar), pp. 157–187. Oxford: Clarendon Press.
Monteith, J. L. 1973 *Principles of environmental physics*. London: Edward Arnold.
Pahor, S. 1985 On the $-\frac{3}{2}$ power thinning law in plant ecology. *J. theor. Biol.* **112**, 535–537.
Papoulis, A. 1984 *Probability, random variables, and stochastic processes* (2nd edn). Singapore: McGraw-Hill.
Perry, D. A. 1984 A model of physiological and allometric factors in the self-thinning curve. *J. theor. Biol.* **106**, 383–401.
Pickard, W. F. 1983 Three interpretations of the self-thinning rule. *Annls Bot.* **51**, 749–757.
Richards, F. J. 1959 A flexible growth function for empirical use. *J. exp. Bot.* **10**, 290–300.
Steingraeber, D. A. & Waller, D. M. 1986 Non-stationarity of tree branching patterns and bifurcation ratios. *Proc. R. Soc. Lond.* B **228**, 187–194.
Stephenson, G. 1971 *Inequalities and optimal problems in mathematics and the sciences*. London: Longman.
Steward, F. C. 1968 *Growth and organisation in plants*. London: Addison-Wesley.
Shinozaki, K. & Kira, T. 1956 Intraspecific competition among higher plants. VII. Logistic theory of the C–D effect. *J. Polytech. Inst., Osaka City Univ.* D **7**, 35–72.
Takadi, Y. & Shidei, T. 1959 Studies on the competition of forest trees. *J. Jap. For. Soc.* **41**, 341–349.
Watkinson, A. R. 1980 Density-dependence in single species populations of plants. *J. theor. Biol.* **80**, 344–357.
Weiner, J., Berntson, G. M. & Thomas, S. C. 1990 Competition and growth form in a woodland annual. *J. Ecol.* **78**, 459–469.
Weller, D. E. 1987 A reevaluation of the $-\frac{3}{2}$ power rule of plant self-thinning. *Ecol. Monogr.* **57** (1), 23–43.
Westoby, M. 1984 The self-thinning rule. *Adv. Ecol. Res.* **14**, 167–226.
Westoby, M. & Howell, J. 1986 Influence of population structure on self-thinning of plant populations. *J. Ecol.* **74**, 343–359.
White, J. 1980 In *Demography and evolution in plant populations* (ed. O. T. Solbrig). *Bot. Monogr.* **15**, p. 35.
White, J. 1981 The allometric interpretation of the self-thinning rule. *J. theor. Biol.* **89**, 475–500.
White, J. & Harper, J. C. 1970 Correlated changes in plant size and number in plant populations. *J. Ecol.* **58**, 467–485.
Whittaker, R. H. & Woodwell, G. M. 1968 Dimensions and production relations of trees and shrubs in the Brookhaven Forest, New York. *J. Ecol.* **56**, 1–25.
Yoda, K., Kira, T., Ogawa, H. & Hozumi, K. 1963 Self-thinning in overcrowded pure stands under cultivated and natural conditions. *J. Biol. Osaka City Univ.* **14**, 107–129.

Communicated by J. L. Harper; typescript received 28 March 1991; accepted 8 April 1991

APPENDIX 1. CANOPY ENVELOPE GEOMETRY

Because the radius R, height H, and the shape parameter A for each canopy envelope are necessary components in the evaluation of the non-dimensional biomass μ, these have been grouped and classified so as to facilitate comparisons with field observations. Figure A 1.1 (*a*) shows the essential features of canopy envelope geometry together with the dimensions needed to specify this.

All of the shapes are assumed to have rotational symmetry about the vertical axis and plane bases of either finite or zero area. Cases without either of these properties may be dealt with where required. The contour of the envelope is specified in terms of the functions

$$y = f(x) \quad \text{or} \quad x = g(y), \tag{A 1.1}$$

so that the surface area S is given by

$$S = 2\pi \int_{H_0}^{H} g(y)[1 + \{g'(y)^2\}]\,\mathrm{d}y + \pi R_0^2, \tag{A 1.2}$$

where the primes denote differentiation, and the volume enclosed by this area by

$$V = \pi \int_{H_0}^{H} \{g(y)\}^2 \mathrm{d}y. \tag{A 1.3}$$

The plant cylinder has the surface area S_c, defined in

PHILOSOPHICAL TRANSACTIONS OF THE ROYAL SOCIETY B BIOLOGICAL SCIENCES
PHILOSOPHICAL TRANSACTIONS OF THE ROYAL SOCIETY B BIOLOGICAL SCIENCES

Downloaded from rstb.royalsocietypublishing.org

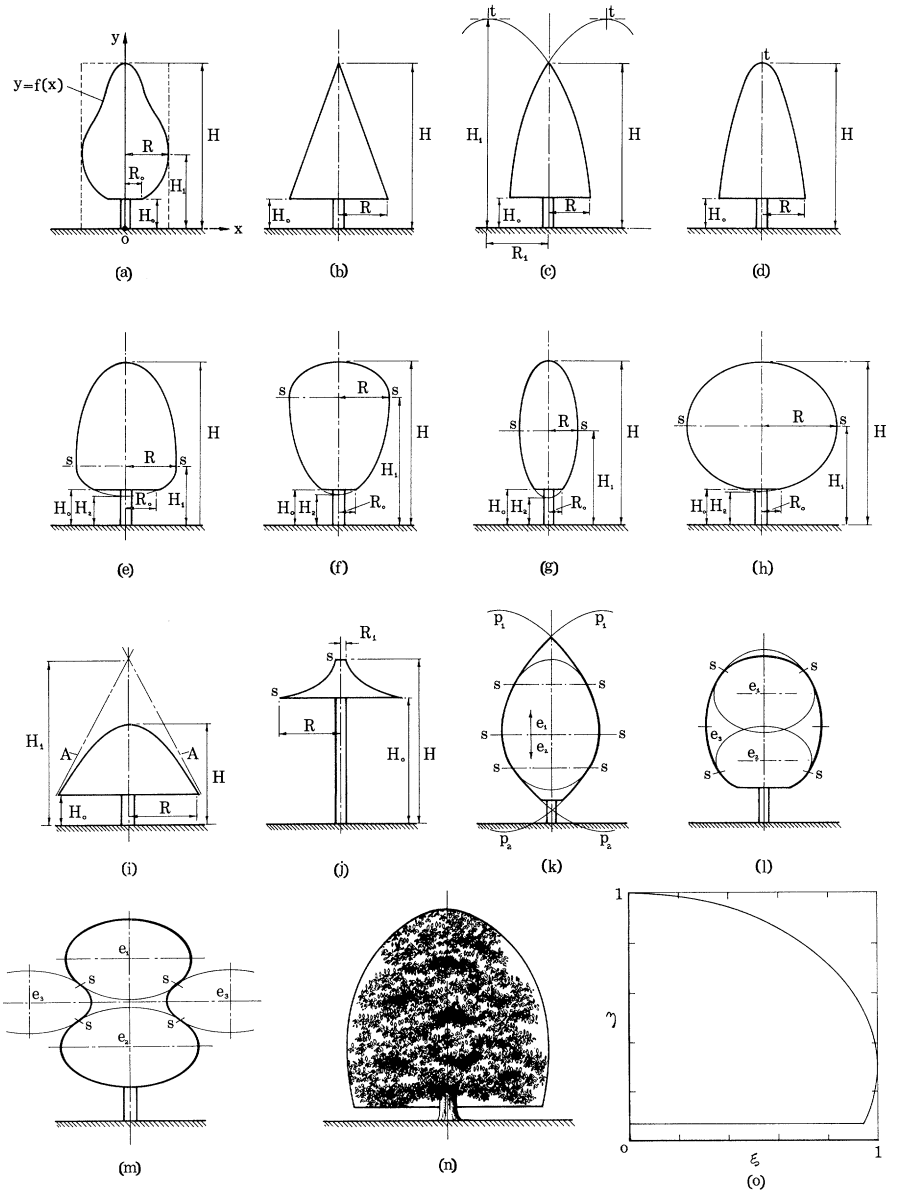

Figure A 1.1. The figure shows the principal features and dimensions required for the calculation of the canopy shape parameter Λ, together with a preliminary classification of canopies and an example fitted envelope.

(a) General canopy geometry and the coordinate system needed to describe it. The broken lines represent the outline of the plant cylinder.

(b–j) Primary shapes. (b) Right-circular conical. (c) Convex offset-parabolic; the vertices of the defining parabolae are at t. (d) Parabolic; this is formed by a single parabola with vertex at t and is a special case of (c) with $H_1 = H$ and $R_1 = 0$. (e–h) Bi-elliptic; the four possible forms having surface joins s on the principal axes are shown. (i) Hyperbolic, with asymptotes A. (j) Catenoidal; single-layered form with top radius R_1 and end-point s on the extremal curve.

(k–m) Higher-order compound shapes. For each of the cases shown the surface joins at s, made between any upper and lower contour pair, are matched for contour radius and surface slope. (k) Compound conic; this is made up of offset parabolae p_1 and p_2, together with upper and lower ellipses e_1 and e_2. (l) Triple elliptic; made up of upper and lower ellipses e_1 and e_2, and an embracing ellipse e_3. (m) Inflected profile, shown made up of upper and lower ellipses e_1 and e_2, with a toroidal ellipse e_3 providing the reverse curvature. (n) Example canopy envelope and, at (o), the non-dimensional form of this.

(1), so that (A 1.2) may be expressed in the preferred non-dimensional form required for the evaluation of Λ as

$$S/S_c = \left\{2\int_{\eta_0}^{1} \xi(1+\lambda^2\xi'^2)^{\frac{1}{2}}\mathrm{d}\eta + K_0\lambda\xi_0^2\right\}/(2+\lambda), \quad \text{(A 1.4)}$$

where $\xi = x/R$, $\eta = y/H$, $\xi_0 = R_0/R$, $\lambda = R/H$, $\eta_0 = H_0/H$ and $K_0 = 1-\exp(k_0\eta_0/\lambda)$, where k_0 is an attenuation constant. K_0 describes the effectiveness of the undersurface area of the canopy in converting reflected radiant energy into biomass and ensures correct matching of surface area with that of the plant cylinder when $\eta_0 = 0$. The corresponding non-dimensional form for the volume (A 1.3) is

$$V/V_c = \int_{\eta_0}^{1} \xi^2\mathrm{d}\eta. \quad \text{(A 1.5)}$$

Quite a large variety of the envelopes enclosing the

Downloaded from rstb.royalsocietypublishing.org

canopies of plants of many shapes and sizes may be described quite well by suitable choice of the defining constants for the contours in the following list, for which corresponding examples are shown in figure A 1.1, (*b–m*). All of the shapes considered involve conic sections, which were chosen because of the analytical advantages afforded when dealing with the integrals (A 1.2) and (A 1.3). Some of the shapes are like those considered by Assmann (1970) and mentioned by Gates *et al.* (1979).

Primary shapes:

(i) Right-circular conical.
(ii) Convex offset-parabolic.
(iii) Bi-elliptic.
(iv) Hyperbolic.
(v) Catenoidal.

Higher-order compound shapes:

(vi) Compound conic.
(vii) Triple elliptic.
(viii) Inflected profile.

The right-circular conical shapes (i) are the simplest ones and amount to a limiting case of the more general convex offset parabolic canopies (ii), which, taken together with the bi-elliptic form (iii), give a fairly wide coverage of a most useful kind. The hyperbolic sections (iv) complement the parabolic ones (ii); the catenoidal surface is an extremal curve defining the surface of revolution of minimum area for an arc joining the end points *s* shown in figure A 1.1 (j). Such a surface has significance when minimum rates of evaporation from surfaces tissues are vital for survival. The compound conic sections (vi), the triple-elliptic sections (vii), and the inflected profiles (viii) offer refined means of construction for an extremely wide range of canopy geometries.

For the primary shapes listed above the contour descriptions, surfaces and volumes are quoted in suitable non-dimensional form in Table 1. The compound shapes have not been included in the table because of the rather wide range of combinations possible in the matching of contour slopes and radii at the joins in the construction of these composite contours. It is appropriate to deal with such cases individually as required.

Example calculation

An example canopy envelope, together with the corresponding non-dimensional form of this curve, are shown in figure A 1.1 (n, o). These were derived for the following values of dimensions and parameters:

Canopy dimensions:

$H = 25.9\,\mathrm{m}, \quad H_1 = 7.62\,\mathrm{m}, \quad H_0 = 1.83\,\mathrm{m},$
$H_2 = -10.7\,\mathrm{m}, \quad R = 12.2\,\mathrm{m},$

Dimensional envelope:

$$(x/12.2)^2 + (y-7.62)^2/(18.3)^2 = 1.$$

Non-dimensional parameters:

$\lambda = R/H = 0.471, \quad \eta_1 = H_1/H = 0.294,$
$\eta_0 = H_0/H = 0.0706, \quad \eta_2 = H_2/H = -0.412,$
$\xi_0 = 0.949, \quad K_0 = 0.139, \quad k_0 = 1.$

Non-dimensional envelope:

$$\xi^2 + (\eta - 0.294)^2/(0.706)^2 = 1.$$

Table 1. *Contour descriptions, surfaces and volumes of primary shapes*

(Shape parameter: $\Lambda = (S/S_c)\,(V/V_c)$.)

(*a*) Right-circular conic
Specified by: R, H, H_0
Envelope: $\xi = 1-(\eta-\eta_0)/(1-\eta_0)$
Area ratio: $S/S_c = [\{\lambda^2+(1-\eta_0)^2\}^{\frac{1}{2}}+K_0\lambda]/(2+\lambda)$
Volume ratio: $V/V_c = (1-\eta_0)/3$

(*b*) Convex offset-parabolic
Specified by: R, R_1, H, H_0
Envelope: $\xi = -\xi_1+\{\xi_1^2+(1-\eta)/a_1\}^{\frac{1}{2}}, \quad \eta_1 = 1+a_1\xi_1^2$
Area ratio: $S/S_c = (2I+K_0\lambda)/(2+\lambda)$
Volume ratio: $V/V_c = (1-\eta_0)\,[4\xi_1\{\xi_1^3-(\xi_1+1)^3\}/\{3(1+2\xi_1)\}+2\xi_1^2+(1+2\xi_1)/2]$
where
$I = a_1\xi_1^3[\sqrt{a_3}-\sqrt{a_4}\sqrt{a_5}+a_2\ln\{(1+\sqrt{a_3})/(\sqrt{a_4}+\sqrt{a_5})\}-2(a_3^{\frac{3}{2}}-a_5^{\frac{3}{2}})/3]$
$a_1 = (1-\eta_0)/(1+2\xi_1), \quad a_2 = \{\lambda/(2a_1\xi_1)\}^2, \quad a_3 = 1+a_2,$
$a_4 = 1+a_6, \quad a_5 = a_3+a_6, \quad a_6 = (1+2\xi_1)/\xi_1^2.$
Special case:
$\xi_1 = 0, \quad H_1 = H$
$I = [\{4(1-\eta_0)^2+\lambda^2\}^{\frac{3}{2}}-\lambda^3]/\{12(1-\eta_0)^2\}$
$V/V_c = (1-\eta_0)/2$

(*c*) Bi-elliptic: upper and lower contour joins on principal axes
Specified by: R, R_0, H, H_0, H_1, H_2
Envelope:
Upper ellipse: $\xi^2+(\eta-\eta_1)^2/(1-\eta_1)^2 = 1$
Lower ellipse: $\xi^2+(\eta-\eta_1)^2/(\eta_1-\eta_2)^2 = 1$
Area ratio: $S/S_c = \{2(I_u+I_l)+K_0\lambda\xi_0^2\}/(2+\lambda)$
Volume ratio: $V/V_c = 2(1-\eta_1)/3+(\eta_1-\eta_0)\,[1-(\eta_1-\eta_0)^2/\{3(\eta_2-\eta_1)^2\}]$
where
$I_u = (1-\eta_1)\,\{\sqrt{a_1}+(1/\sqrt{a_2})\ln(\sqrt{a_2}+\sqrt{a_1})\}/2, \quad a_2 > 0,$

Downloaded from rstb.royalsocietypublishing.org

Table 1. (*cont*)

$I_u = (1-\eta_1)\{\sqrt{a_1}+(1/\sqrt{a_3})\arcsin(\sqrt{a_3})\}/2, \quad a_3 > 0,$
$I_l = (\eta_1-\eta_2)\{a_5\sqrt{a_6}+(1/\sqrt{a_4})\ln(a_5\sqrt{a_4}+\sqrt{a_6})\}/2, \quad a_4 > 0,$
$I_l = (\eta_1-\eta_2)\{a_5\sqrt{a_6}+(1/\sqrt{a_7})\arcsin(a_5\sqrt{a_7})\}/2, \quad a_7 > 0,$
$a_1 = \lambda^2/(1-\eta_1)^2, \quad a_2 = a_1-1, \quad a_3 = -a_2, \quad a_4 = \lambda^2/(\eta_1-\eta_2)^2-1$
$a_5 = (\eta_1-\eta_0)/(\eta_1-\eta_2), \quad a_6 = 1+a_4a_5^2, \quad a_7 = -a_4$

(*d*) Hyperbolic

Specified by:	R, H, H_0, H_1
Envelope:	$\{(a_1-\eta)^2-(a_2\xi)^2\}/(a_1-1)^2 = 1$
Asymptotes:	$\eta = \pm a_2\xi+a_1$
Area ratio:	$S/S_c = (2I+K_0\lambda)/(2+\lambda)$
Volume ratio:	$V/V_c = \{(a_1-\eta_0\}^3-(a_1-1)^2(a_1-3\eta_0+2)\}/(3a_2^2)$

where

$I = \{a_4/(2a_2^2)\}\{b_1(b_1^2-a_5^2)^{\frac{1}{2}}-b_2(b_2^2-a_5^2)^{\frac{1}{2}}+a_5^2\ln(b_7)\},$
$a_1 = H_1/H, \quad a_2^2 = (1-\eta_0)(2a_1-1-\eta_0), \quad a_3 = a_2(a_1-1),$
$a_4 = (a_2^2+\lambda^2)^{\frac{1}{2}}, \quad a_5 = a_3/a_4, \quad a_6 = a_1+a_5, \quad a_7 = a_1-a_5$
$b_1 = a_1-\eta_0, \quad b_2 = a_1-1, \quad b_3 = a_6-\eta_0, \quad b_4 = a_6-1,$
$b_5 = a_7-\eta_0, \quad b_6 = a_7-1$
$b_7 = (\sqrt{b_4}+\sqrt{b_6})(\sqrt{b_3}-\sqrt{b_5})/\{(\sqrt{b_4}-\sqrt{b_6})(\sqrt{b_3}+\sqrt{b_5})\}$

(*e*) Catenoidal

Specified by:	R, R_1, H, H_0
Envelope:	$\xi = \xi_1\cosh\{(1-\eta)/(\lambda\xi_1)\}$
	$\eta_0 = 1-\lambda\xi_1\,\mathrm{arcosh}\,(1/\xi_1)$
Area ratio:	$S/S_c = \{2I+\lambda(K_0+\xi_1^2)\}/(2+\lambda)$
Volume ratio:	$V/V_c = \xi_1 I$
where	$I = [\xi_1(1-\eta_0)+\lambda\{(1+\xi_1)(1-\xi_1)\}^{\frac{1}{2}}]/2$

From the formulae of Table 1 (*c*):

$S/S_c = 0.716, \quad V/V_c = 0.687, \Lambda = 0.492.$

APPENDIX 2. CALCULATION OF PACKING COEFFICIENTS

In determining the packing coefficient C_p for hexagonal and square arrangements on the plane of cultivation it is convenient to use the coordinate systems of figure A 2.1 (i, ii), wherein the location of each plant cylinder centre is defined in terms of integer multiples mR and nR of the plant cylinder radius R. By allowing the solar cylinder radius R_∞ to vary, the coefficient C_p is evaluated by using the ratio of the shaded areas in figure A 2.1 (i, ii), to πR_∞^2. The shaded areas include whole plant cylinders, and portions of plant cylinders, and the numbers S_m of whole cylinders in regions with upper coordinate limits (n, n) inclusive is given by $S_m = S_0+S_n$, where $S_0 = \frac{1}{12}$ for hexagonal packing, and $S_0 = \frac{1}{8}$ for square, with

$$S_n = n(n+2)/8, \quad n = 2, 4, 6, \ldots, \qquad \text{(A 2.1)}$$

in both cases. The corresponding number of cylinder centres included in each of these packing arrangements is $(n+2)(n+4)/8$. Where only a portion of a plant cylinder lies within the boundary of the solar cylinder, as in figure A 2.1 (iii), the auxiliary coordinate system (r, s) shown is of use in evaluating the required shaded area.

The non-dimensional radial distance from the centre of the solar cylinder to the centre P of an arbitrarily selected plant cylinder is $\lambda_r M_1$ for hexagonal packing, and $\lambda_r M_2$ for square, where $\lambda_r = R/R_\infty$, and

$$M_1 = (m^2+n^2+mn)^{\frac{1}{2}} \quad \text{and} \quad M_2 = (m^2+n^2)^{\frac{1}{2}}. \qquad \text{(A 2.2)}$$

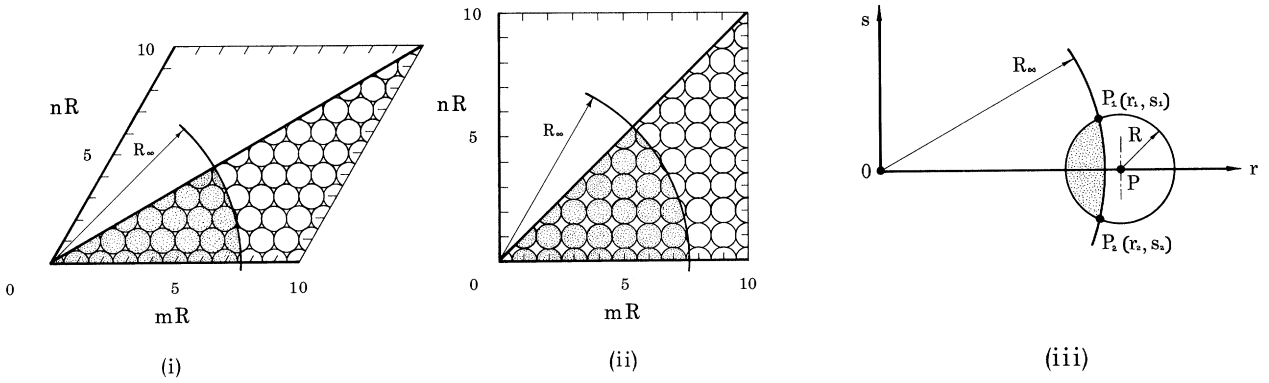

Figure A 2.1. Coordinate systems used for defining the locations of plant cylinder centres and for the evaluation of the packing coefficient C_p for plant cylinders of radius R in a solar cylinder of radius R_∞. (i) The oblique coordinate system (mR, nR) used for hexagonal packing. (ii) The orthogonal system (mR, nR) used for square packing. (iii) The auxiliary coordinate system (r, s) used for determining the areas of the shaded portion of the plant cylinders with centre at P and not wholly included in the solar cylinder.

Downloaded from rstb.royalsocietypublishing.org

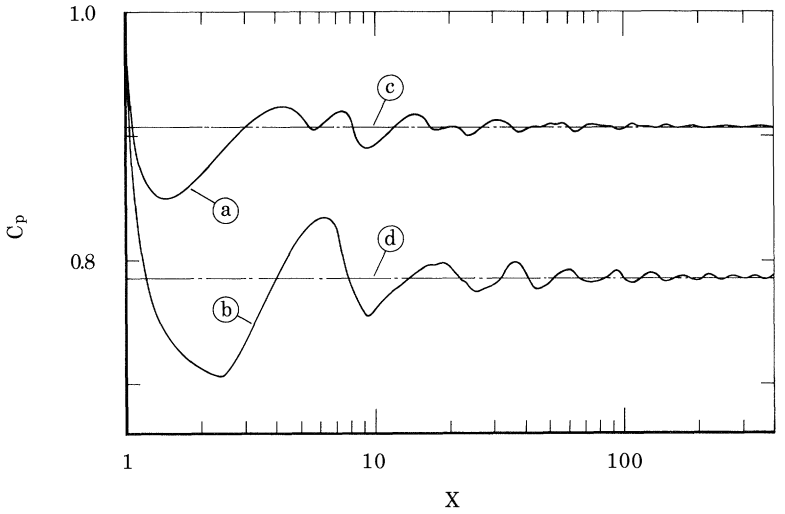

Figure A 2.2. The variation of the packing coefficient C_p with numbers X of plant cylinders within the solar cylinder. (a) Close-packed hexagonal. (b) Close-packed square. (c) Close-packed hexagonal; infinite array for which $C_p = (\pi\sqrt{3})/6$. (d) Close-packed square; infinite array for which $C_p = \pi/4$.

The coordinates of intersection of the peripheries of the solar and plant cylinders at P_1 and P_2 are therefore

$$r_\alpha/R_\infty = q \quad \text{and} \quad s_\alpha/R_\infty = \pm(1-q^2)^{\frac{1}{2}}, \tag{A 2.3}$$

where $q = (1+p^2-\lambda_r^2)/(2p)$, $p = \lambda_r M_\alpha$; $\alpha = 1, 2$, and the positive and negative signs in s_α/R_∞ correspond to $\alpha = 1$ and $\alpha = 2$ respectively. The shaded area A of figure A 2.1 (iii) is determined using

$$A = 2\int_{r_1-R}^{r_1} s\,\mathrm{d}r + 2\int_{r_1}^{R_\infty} s\,\mathrm{d}r, \tag{A 2.4}$$

to obtain

$$A/(\pi R_\infty^2) = [u(\lambda_r^2-u^2)^{\frac{1}{2}} - q(1-q^2)^{\frac{1}{2}} + \arccos(q) + \lambda_r^2\{\pi - \arccos(v)\}]/\pi, \tag{A 2.5}$$

where $u = q-p$, $v = u/\lambda_r$. In evaluating the integrals separate account must be taken of those cylinders with centres in the vicinity of the sector and solar cylinder boundaries and for which only a part of each lies in the region of integration. Some values calculated for C_p are shown in figure A 2.2.

APPENDIX 3. CALCULATION OF DIFFUSION AT GROWTH PHASE BOUNDARIES

To estimate the magnitude and extent of the rounding off that occurs as the growth life-line approaches the plastic and self-thinning lines the expected value $\mathrm{E}[X(\tau)]$ of X at time τ is determined first so as to define the projection of the growth life-line on the $\tau-X$ plane corresponding to a given starting value X_0 of X. The expected value $\mathrm{E}[\mu(\tau, X)]$ of the mass μ associated with paired values of the coordinates τ and X on this growth life-line then follows at once.

Figure A 3.1 shows the coordinates used for evaluating the growth life-line. For a given starting value

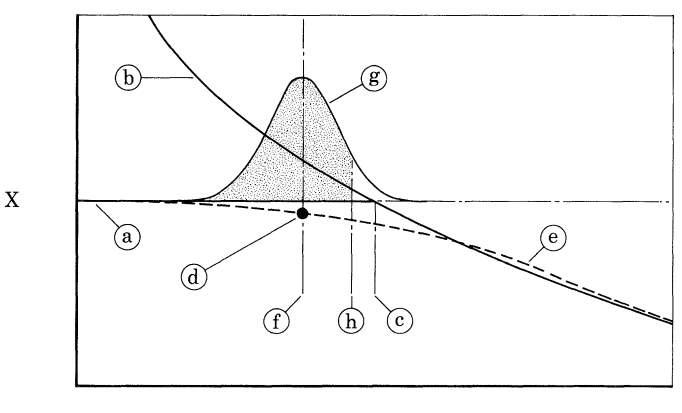

Figure A 3.1. Coordinates and quantities used in the calculation of growth life-lines. (a) The horizontal line denotes the initial value of the planting density $X = X_0$. (b) The self-thinning line. Note that without any diffusion of properties across the growth phase boundaries, (a) and (b) between them define the growth life-line. (c) Point of intersection of (a) and (b) at $\tau = \tau_t$. (d) Point with coordinates $(\tau, \mathrm{E}[X(\tau)])$ on the growth life-line (e) with diffusion of properties at the growth phase boundaries. (f) The line of symmetry of the Gaussian normal distribution (g) which is centred on (d). (h) $\tau = \tau_1$, where τ_1 is the dummy variable of integration required for the evaluation of $\mathrm{E}[X(\tau)]$ using (A 3.1).

Downloaded from rstb.royalsocietypublishing.org

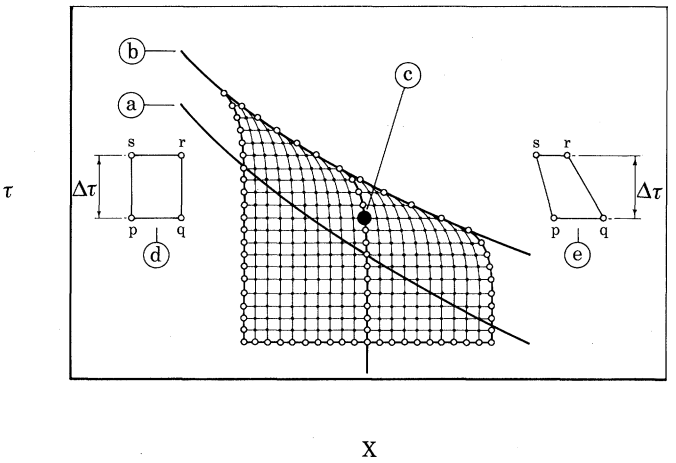

Figure A 3.2. The integration lattice used for the evaluation of $\mathrm{E}[X(\tau)]$ and $\mathrm{E}[\mu(\tau, X)]$ using (A 3.3) and (A 3.4). The open circles indicate points on the growth life-line being calculated and also the boundaries of the integration lattice. (a) The plastic line. (b) The self-thinning line. (c) This is the point (τ, X) on the growth life-line for which $\mathrm{E}[\mu(\tau, X)]$ was determined at each stage of the integration. (d), (e) Typical lattice elements. $\Delta\tau$ was assigned the same value in all cases for each of the 10 node spacings on either side of τ.

X_0 of the planting density the expectation $\mathrm{E}[X(\tau)]$ at time τ associated with the probability density function $F_1(\tau)$ is such that

$$\mathrm{E}[X(\tau)] = X_0 \int_{-\infty}^{\tau_t} F_1(\tau_1)\,\mathrm{d}\tau_1 + \int_{\tau_t}^{\infty} X(\tau_1)\,F_1(\tau_1)\,\mathrm{d}\tau_1, \tag{A 3.1}$$

where

$$F_1(\tau_1) = a_1 \exp(-f_1/2), \quad a_1 = 1/(2\pi\sigma_1),$$
$$\sigma_1^2 = \mathrm{E}[(\tau_1-\tau)^2], \quad f_1 = (\tau_1-\tau)^2/\sigma_1,$$

and τ_1 is the dummy variable of integration.

For the mass μ, the expectation $\mathrm{E}[\mu(\tau, X)]$, for given values of τ and the corresponding value of X, is

$$\mathrm{E}[\mu(\tau, X)] = \int_{-\infty}^{\tau_p}\int_{1}^{X_p} \mu_1(\tau_2, X_2)\,F_2(\tau_2, X_2)\,\mathrm{d}\tau_2\,\mathrm{d}X_2 + \int_{\tau_p}^{\infty}\int_{X_p}^{\infty} \mu_2(\tau_2, X_2)\,F_2(\tau_2, X_2)\,\mathrm{d}\tau_2\,\mathrm{d}X_2, \tag{A 3.2}$$

where $F_2(\tau_2, X_2)$ is the bivariate Gaussian probability density function, representing the statistical uncertainty of the growth state of the mean, with dummy variables of integration τ_2 and X_2, and for which

$$F_2(\tau_2, X_2) = (1/a_2)\exp(-f_2), \quad f_2 = (f_3 - f_4 + f_5)/a_3,$$
$$f_3 = (\tau_2-\tau)^2/\sigma_2^2, \quad f_4 = 2\sigma_4(\tau_2-\tau)(X_2-X)/(\sigma_2\sigma_3),$$
$$f_5 = (X_2-X)^2/\sigma_3^2,$$
$$\sigma_2^2 = \mathrm{E}[(\tau_2-\tau)^2], \quad \sigma_3^2 = \mathrm{E}[(X_2-X)^2],$$
$$\sigma_4 = \mathrm{E}[(\tau_2-\tau)(X_2-X)]/(\sigma_2\sigma_3),$$
$$a_2 = 2\pi\sigma_2\sigma_3(1-\sigma_4^2)^{\frac{1}{2}}, \quad a_3 = 2(1-\sigma_4^2).$$

Because of the difficulties of dealing with (A 3.1) and (A 3.2) analytically, the expectations $\mathrm{E}[X(\tau)]$ and $\mathrm{E}[\mu(\tau, X)]$ were evaluated by forming Riemann sums for elements $\Delta\tau$ and $\Delta A = \Delta\tau\,\Delta X$. For the τ–X plane, (A 3.1) was replaced with

$$\mathrm{E}[X(\tau)] = \Sigma\, X(\tau)\,F_1(\tau)\,\Delta\tau / \Sigma\, F_1(\tau)\,\Delta\tau, \tag{A 3.3}$$

and calculations made with equal increments $\Delta\tau$ to determine the location of the node points on a 20×20 lattice, arranged symmetrically with respect to the reference point (c), as shown in figure A 3.2.

For the growth surface, (A 3.2) was replaced with

$$\mathrm{E}[\mu(\tau, X)] = \Sigma\Sigma\,\mu_\alpha(\tau, X)\,F_2(\tau, X)\,\Delta A / \Sigma\Sigma\,F_2(\tau, X)\Delta A, \quad \alpha = 1, 2, \tag{A 3.4}$$

and calculations made with the life-line projection coordinates established for the curved lattice. In forming the sum (A 3.4) the contributions from each four-cornered element (figure A 3.2 (d, e)) was taken as the arithmetic mean of that from each of the corners p, q, r, and s such that

$$\mu(\tau, X)\,F_2(\tau, X)\,\Delta A = \tfrac{1}{4}\{\mu(\tau_\mathrm{p}, X_\mathrm{p})\,F_2(\tau_\mathrm{p}, X_\mathrm{p}) + \mu(\tau_\mathrm{q}, X_\mathrm{q})\,F_2(\tau_\mathrm{q}, X_\mathrm{q}) + \mu(\tau_\mathrm{r}, X_\mathrm{r})\,F_2(\tau_\mathrm{r}, X_\mathrm{r}) + \mu(\tau_\mathrm{s}, X_\mathrm{s})\,F_2(\tau_\mathrm{s}, X_\mathrm{s})\}\,\Delta A, \tag{A 3.5}$$

and

$$F_2(\tau, X)\,\Delta A = \tfrac{1}{4}\{F_2(\tau_\mathrm{p}, X_\mathrm{p}) + F_2(\tau_\mathrm{q}, X_\mathrm{q}) + F_2(\tau_\mathrm{r}, X_\mathrm{r}) + F_2(\tau_\mathrm{s}, X_\mathrm{s})\}\Delta A, \tag{A 3.6}$$

where

$$\Delta A = \Delta\tau(\Delta X_\mathrm{pq} + \Delta X_\mathrm{sr})/2, \quad \Delta X_\mathrm{pq} = X_\mathrm{q} - X_\mathrm{p},$$
$$\Delta X_\mathrm{sr} = X_\mathrm{r} - X_\mathrm{s}.$$